Supporting Information

Side-Chain Regulated Topology of 2D Covalent Organic Frameworks and Its Impact on Photocatalytic Synthesis of H_2O_2

Shuai Sun,[a,b] Chao-Qin Han*[,b] Jia-Xin Guo,[a,b] Lei Wang,[b] Ze-Yang Wang,[b] Gonghao Lu*[,a] and Xiao-Yuan Liu,*[,b]

[a] School of Chemical Engineering, University of Science and Technology Liaoning, 185 Qianshan Zhong Road, Anshan, 114051, P. R. China

[b] Hoffmann Institute of Advanced Materials, Shenzhen Polytechnic University, 7098 Liuxian Blvd, Nanshan District, Shenzhen, 518055, P. R. China

Chemicals

4,7-dibromobenzo[c][1,2,5]thiadiazole，tri-t-butylphosphonium tetrafluoroborate, 2,5-diethoxy, 2,5-diethoxyterephthalaldehyde (DETA), 2,5-dipropoxyterephthalaldehyde (DPTA) and 2,5-dibutoxyterephthalaldehyde (DBTA), 2-(dicyclohexylphosphino)-2',4',6'-tri-i-propyl-1,1'-biphenyl, terephthalaldehyde (TPA), tert-butyl carbamate, 2,5-dihydroxyterephthalaldehyde tetrabutylammonium tribromide and cesium carbonate were purchased from Shanghai Bidepharm Co., Ltd. Diphenylamine, trifluoroacetic acid (TFA) and 1,2-dichlorobenzene (*o*-DCB) were purchased from Shanghai Macklin Biochemical Technology Co., Ltd. 1,3,5-trimethylbenzene (Mes) *n*-butanol (*n*-BuOH) and 2,5-dihydroxyterephthalaldehyde (DHTA) were purchased from Shanghai Aladdin Biochemical Technology Co., Ltd. All the other chemicals were obtained from the chemical supplies and used without further purification.

Characterization

Powder X-ray diffraction (PXRD) patterns for synthesized COFs were measured using Bruker D 8 Advance X-ray diffractometer with Cu Kα radiation. Nuclear magnetic resonance (NMR) data were collected using 400 MHz JEOL JNM-ECZ400S. The Steady-state photoluminescent spectra were recorded on FLS1000 spectrofluorometer (Edinburgh Instruments). The UV-vis spectra were recorded on Shimadzu UV-3600 spectrophotometer. The TGA data were obtained using TGA 550 (TA Instruments) analyzer and the samples were heated from room temperature to 800 °C at a ramp rate of 10 °C / min in N_2 atmosphere. Fourier transform infrared (FT-IR) spectra were recorded on a PerkinElmer spectrometer. Scanning electron micrographs (SEM) images were taken using a JEOLJSM-IT800 (SHL). The electron paramagnetic resonance

(EPR) measurements were performed by Bruker EMX-plus.

Photocatalytic H_2O_2 production

5 mg of COFs and 10 mL water were added into a 20 mL glass bottle, then the suspension was well dispersed by sonicating for 30 min. All photocatalytic reactions were conducted in an air atmosphere under the illumination of a 300 W xenon lamp with a UV cut-off filter at 420 nm. After the reaction is completed, 0.5 mL of sample was filtered using 0.22 μM filters. To this solution, 1 mL 0.1 M potassium hydrogen phthalate ($C_8H_5KO_4$) solution and 1 mL 0.4 M/L aqueous potassium iodide (KI) solution was added, and the mixture was allowed to sit for 30 min. Under acidic conditions, photocatalytic generated H_2O_2 molecules reacted with iodide anions (I^-) to produce triiodide anions (I_3^-), which has a strong absorption around 350 nm. The quantity of I_3^- was determined via UV-vis spectroscopy based on the absorbance at 350 nm, which allowed the estimation of the amount of H_2O_2 produced during each reaction.

Photoelectrochemical Measurements

Photoelectrochemical measurements were conducted with a CHI660E (CH Instrument Corp, Shanghai) electrochemical workstation. Firstly, 5 mg of COFs were added into a mixed solution of 500 μL of ethanol and 50 μL of 5 wt% Nafion, which was ultrasonicated until a uniform suspension is obtained. Then, COFs suspension was dropped on the surface of ITO glass and dried at room temperature.

Mott-Schottky measurement

A standard three-electrode system was used with the COF-coated ITO glass as the working electrode, Pt wire as the counter electrode and an Ag/AgCl as a reference electrode. 0.1 M Na_2SO_4 aqueous solution was used as the electrolyte.

Electrochemical impedance measurement (EIS)

A standard three-electrode system was used with the COF-coated ITO glass as the working electrode, Pt wire as the counter electrode and an Ag/AgCl as a reference electrode. 0.1 M KCl and 5 mM [$Fe(CN)_6^{3-}$] mixed aqueous solution was used as the electrolyte.

Photocurrent measurement

A standard three-electrode system was used with the COF-coated ITO glass as the working electrode, Pt wire as the counter electrode and an Ag/AgCl as a reference electrode. 0.5 M Na_2SO_4 aqueous solution was used as the electrolyte.

Rotating disk electrode (RDE) measurements

The rotating disk electrode was used as the substrate for the working electrode. Carbon rods and Ag/AgCl electrodes were used as counter and reference electrodes, respectively. 10 mg COFs were dispersed in a mixture of 0.5 mL ethanol, which was sonicated to obtain a uniform slurry. Then 200 μL samples were taken and added 20 μL Nafion (5 wt%), which was dripped onto the disc electrode and allowed to dry at room temperature. Linear sweep voltammetry (LSV) was obtained at room temperature in O_2-saturated 0.1 M phosphate-buffered saline (PBS, pH = 7) solutions at with a scanning rate of 10 mV s^{-1}. The average number of electrons (n) was calculated by Koutecky-Levich equation

$$\frac{1}{J} = \frac{1}{J_L} + \frac{1}{J_K} + \frac{1}{B_W^{1/2}} + \frac{1}{J_K}$$

$$B = 0.62nFC_0D_0^{2/3}V^{-1/6}$$

where J is the current density, J_K and J_L are the kinetic and diffusion-limiting current densities, ω is the rotating speed (rpm), n is transferred electron number, F is Faraday constant (96485 C

mol^{-1}), C_0 is the bulk concentration of O_2 (1.26×10^{-3} mol cm^{-3}), D_0 is the diffusion coefficient of O_2 (2.7×10^{-5} cm^2 s^{-1}), and v is kinetic viscosity of the electrolyte (0.01 cm^2 s^{-1}).

Rotating ring-disk electrode (RRDE) measurements

RRDE (Rotating Ring-Disk Electrode) measurements were performed using a rotating ring disk system under the illumination of a 300 W Xe lamp. Voltammograms were recorded in a 0.1 M phosphate buffer solution (pH = 7) at room temperature, employing a scan rate of 10 mV s^{-1} and a rotation rate of 1600 rpm. For the detection of O_2, the potential of the ring electrode was set to -0.23 V (vs. Ag/AgCl) under an argon atmosphere. To detect H_2O_2, the potential of the ring electrode was set to 0.6 V (vs. Ag/AgCl).

Photocatalytic evolution of $\cdot O_2^-$

Tetranitroblue tetrazolium chloride (NBT, 2×10^{-4} M, with an absorption maximum at 259 nm) was employed as probe molecules to determine the amount of $\cdot O_2^-$ generated in the photocatalytic reaction. Typically, 1.0 mL NBT stock solution was introduced into our photocatalytic reaction. Suspension was collected at different time intervals and filtrated by 0.22 μm membrane to exclude the influence of COFs for the determination of $\cdot O_2^-$ concentration with UV-Vis spectrophotometer.

The procedure of ^{1}H NMR for digested COFs

3~4 mg completely activated COF powder was digested in the mixture of DCl (20 wt% in D_2O, ~ 50 μL) and DMSO-d_6 (~ 500 μL) or $CDCl_3$ (~ 500 μL), then the mixture was sonicated for 30 min till an clear solution was obtained. The mixture solution (~500 μL) was used directly for ^{1}H NMR to calculate the actual linker ratio in the HIAM-0023-X% COFs compound. All experiments and characterizations were repeated twice. The actual linker ratios in these COF

compounds were calculated based on integrations of resonance peak intensities. The results were showed in Tables S1.

Synthesis of N^4,N^4,N^7,N^7−tetraphenylbenzo[*c*][1,2,5]thiadiazole-4,7-diamine

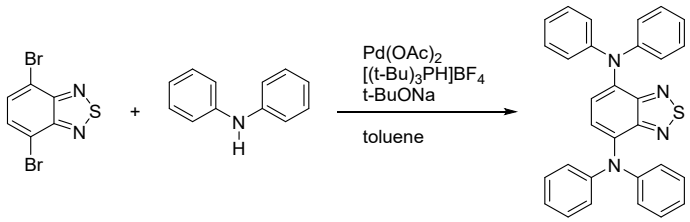

A mixture of 4,7-dibromobenzo[*c*][1,2,5]thiadiazole (5.88 g, 20.0 mmol), diphenylamine (10.15 g, 60.0 mmol), $Pd(OAc)_2$ (224.5 mg, 1.0 mmol), $[(t\text{-}Bu)_3PH]BF_4$ (870.4 mg, 3.0 mmol) and *t*-BuONa (38.44 g, 400.0 mmol) in anhydrous toluene (200 mL) was heated at reflux overnight under a nitrogen atmosphere. After cooling to room temperature, the resulting mixture was diluted with H_2O and ethyl acetate, and the organic layer was washed with brine and water, and dried over Na_2SO_4. The combined organic layer was concentrated under reduced pressure and the residue was purified by silica-gel column chromatography to give a red solid (8.3 g, 88%). ^1H NMR (400 MHz, $CDCl_3$) δ_H (ppm) 7.29-7.26 (8H); 7.11-7.04 (14H).

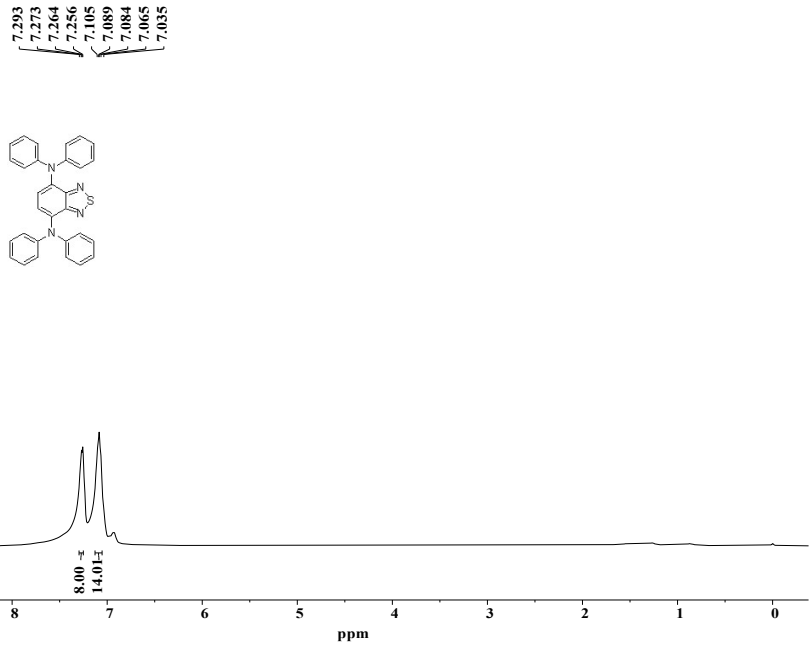

Figure S1. ^{1}H NMR spectrum of *N*^{4},*N*^{4},*N*^{7},*N*^{7}−tetraphenylbenzo[*c*][1,2,5]thiadiazole-4,7-diamine in $CDCl_3$.

Synthesis of *N*^{4},*N*^{4},*N*^{7},*N*^{7}-tetrakis(4-bromophenyl)benzo[*c*][1,2,5]thiadiazole-4,7-diamine

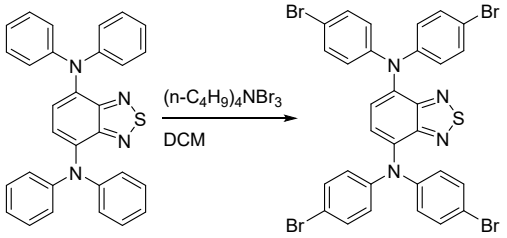

To a solution of *N*^{4},*N*^{4},*N*^{7},*N*^{7}-tetraphenylbenzo[*c*][1,2,5]thiadiazole-4,7-diamine (8.3 g, 17.64 mmol) in dichloromethane (DCM, 600 mL) was added (*n*-C_4H_9)$_4$$Br_3$ (85.04 g, 176.4 mmol) at room temperature. After the mixture was stirred overnight, the resulting mixture was concentrated under reduced pressure. The residue was purified by silica-gel column chromatography to afford target compound as a red solid (5.1 g, 36%). ^{1}H NMR (400 MHz, $CDCl_3$) δ_H (ppm) 7.35 (8H), 7.10 (2H), 6.93 (8H).

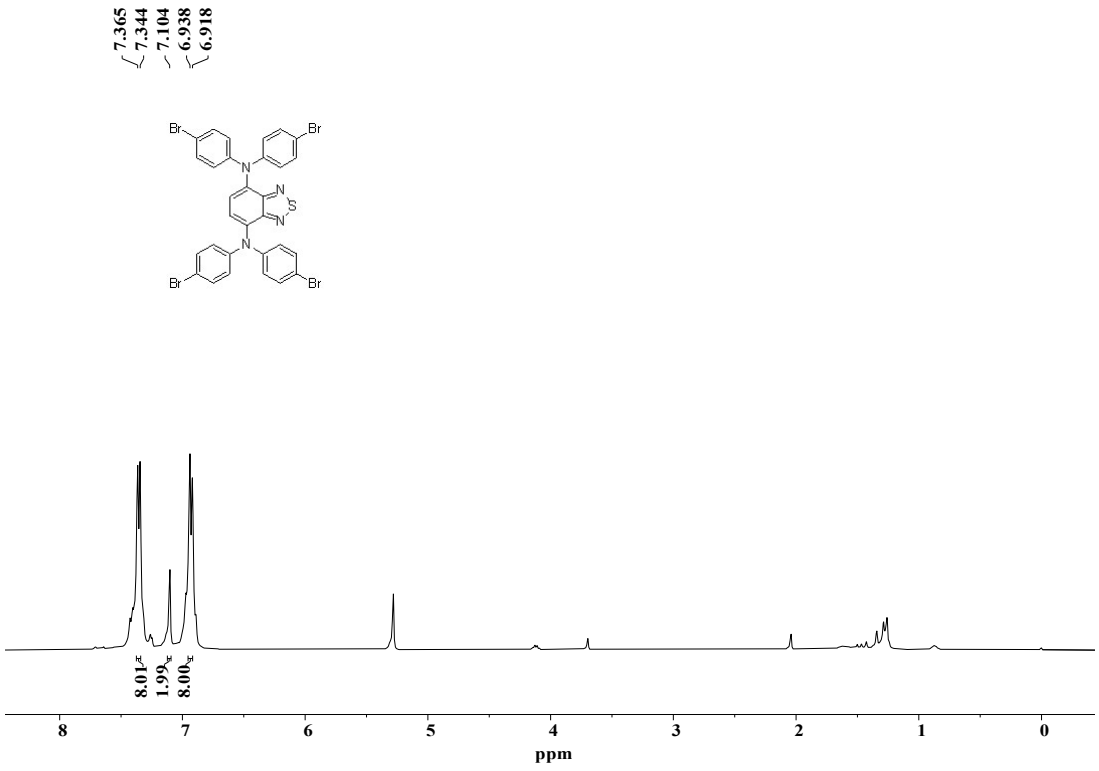

Figure S2. ^{1}H NMR spectrum of compound *N*^{4},*N*^{4},*N*^{7},*N*^{7}-tetrakis(4-bromophenyl) benzo[*c*][1,2,5]thiadiazole-4,7-diamine in $CDCl_3$.

Synthesis of tetra-*tert*-butyl ((benzo[*c*][1,2,5]thiadiazole-4,7-diylbis(azanetriyl)) tetrakis(benzene-4,1-diyl))tetracarbamate

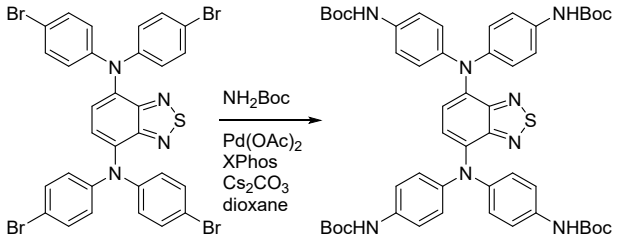

A mixture of *N*^{4},*N*^{4},*N*^{7},*N*^{7}-tetrakis(4-bromophenyl)benzo[*c*][1,2,5]thiadiazole-4,7-diamine (786.2 mg, 1.0 mmol), *t*-butyl carbamate (702.9 mg, 6.0 mmol), $Pd(OAc)_2$ (27 mg, 0.12 mmol), 9,9-dimethyl-4,5-bis(diphenylphosphino)xanthene (XPhos, 171.7 mg, 0.36 mmol) and cesium carbonate (1.82 g, 5.6 mmol) was put in a flask. Under a nitrogen atmosphere, anhydrous dioxane (32 mL) was added through a syringe and the mixture was heated at 100 ˚C overnight. After cooling to room temperature, the mixture was concentrated under reduced pressure. The residue was purified by silica-gel column chromatography to produce target compound as a dark-purple solid (789.9 mg, 84%). ^{1}H NMR (400 MHz, DMSO-d_6) δ_H (ppm) 9.19 (4H), 7.29 (8H), 6.96 (2H), 6.83 (8H), 1.42 (36H). ^{13}C NMR (101 MHz, DMSO-d_6) δ_C (ppm) 153.4, 152.5, 142.7, 135.6, 135.2, 124.5, 124.1, 119.9, 79.4, 28.7.

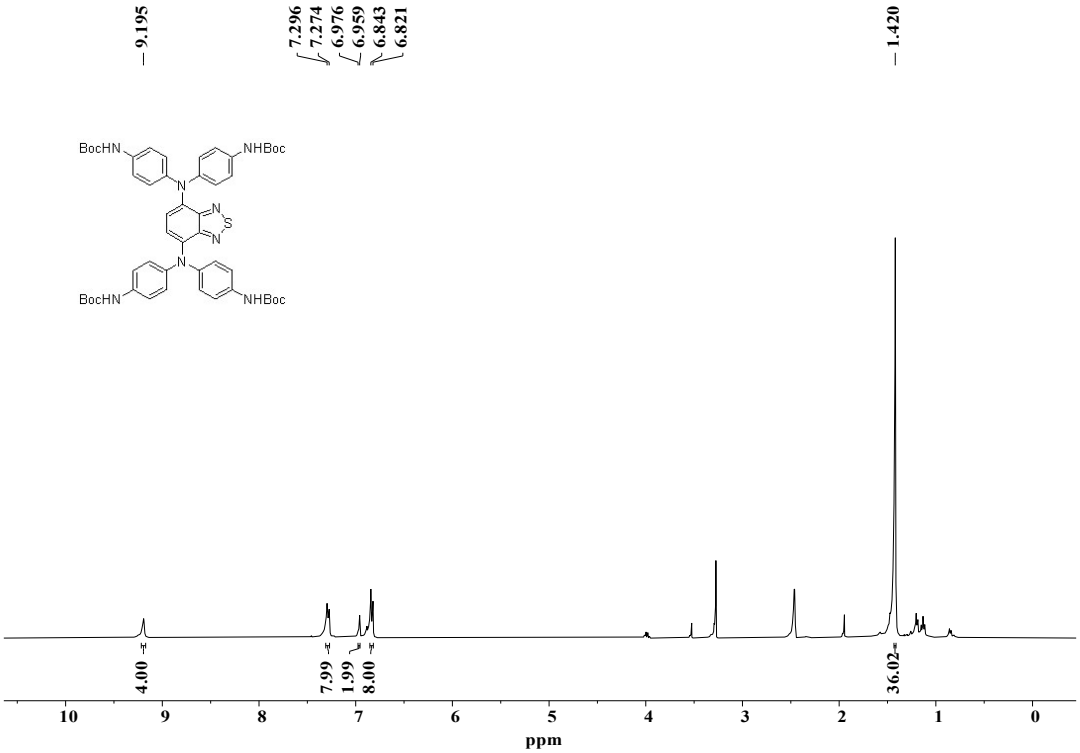

Figure S3. ^{1}H NMR spectrum of compound tetra-*tert*-butyl ((benzo[*c*][1,2,5]thiadiazole-4,7-diylbis(azanetriyl))tetrakis(benzene-4,1-diyl))tetracarbamate in DMSO-d_6.

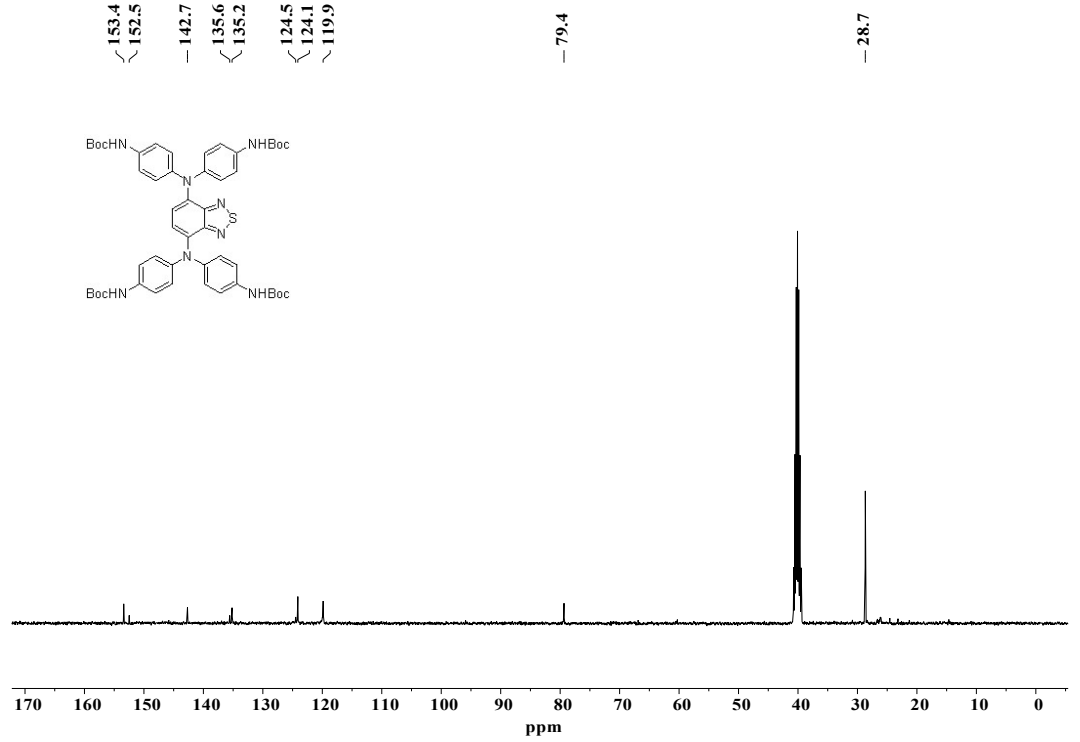

Figure S4. ^{13}C NMR spectrum of compound tetra-*tert*-butyl ((benzo[*c*][1,2,5]thiadiazole-4,7-diylbis(azanetriyl))tetrakis(benzene-4,1-diyl))tetracarbamate in DMSO-d_6.

Synthesis of $N^1,N^{1\prime}$-(benzo[*c*][1,2,5]thiadiazole-4,7-diyl)bis(N^1-(4-aminophenyl) benzene-1,4-diamine) (BTAPA)

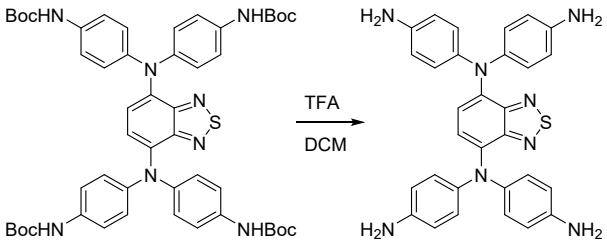

Trifluoroacetic acid (TFA, 50 mL) was dropwisely added to a solution of tetra-*tert*-butyl((benzo[*c*][1,2,5]thiadiazole-4,7-diylbis(azanetriyl))tetrakis(benzene-4,1-diyl)) tetracarbamate in DCM (100 mL) in ice-water bath under nitrogen atmosphere. After the mixture was stirred another 1 h at room temperature, the solvent was removed under reduced pressure. The residue was diluted with DCM and the organic layer was washed with $NaHCO_3$ and 0.1 M NaOH, brine and water. The combined organic layers were dried over Na_2SO_4 and the solvent was removed under reduced pressure. The residue was purified by silica-gel column chromatography to give $N^1,N^{1\prime}$-(benzo[*c*][1,2,5]thiadiazole-4,7-diyl)bis(N^1-(4-aminophenyl)benzene-1,4-diamine) (BTAPA) as a black solid (1.17 g, 69%). ^{1}H NMR (400 MHz, $CDCl_3$) δ_H (ppm) 6.86-6.82 (10H), 6.57 (8H), 3.53 (8H). ^{13}C NMR (101 MHz, $CDCl_3$) δ_C (ppm) 152.1, 141.9, 140.5, 135.7, 125.3, 122.3, 116.1.

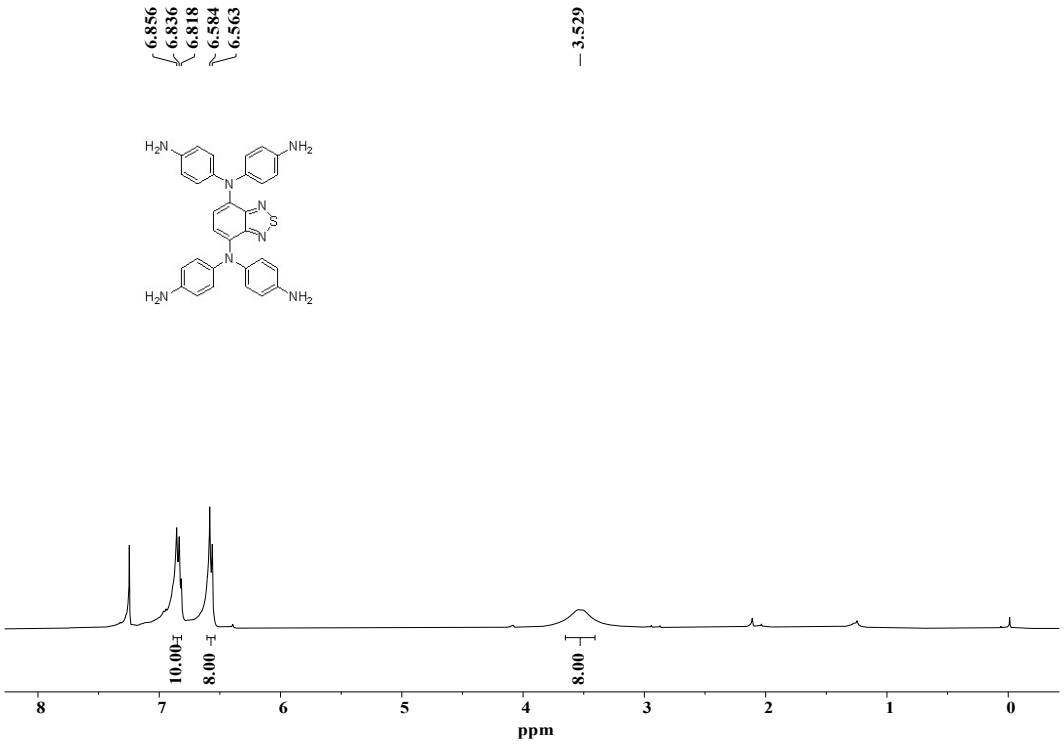

Figure S5. ^{1}H NMR spectrum of compound N^{1},N^{1}'-(benzo[*c*][1,2,5]thiadiazole-4,7-diyl)bis(N^{1}-(4-aminophenyl)benzene-1,4-diamine) (BTAPA) in $CDCl_3$.

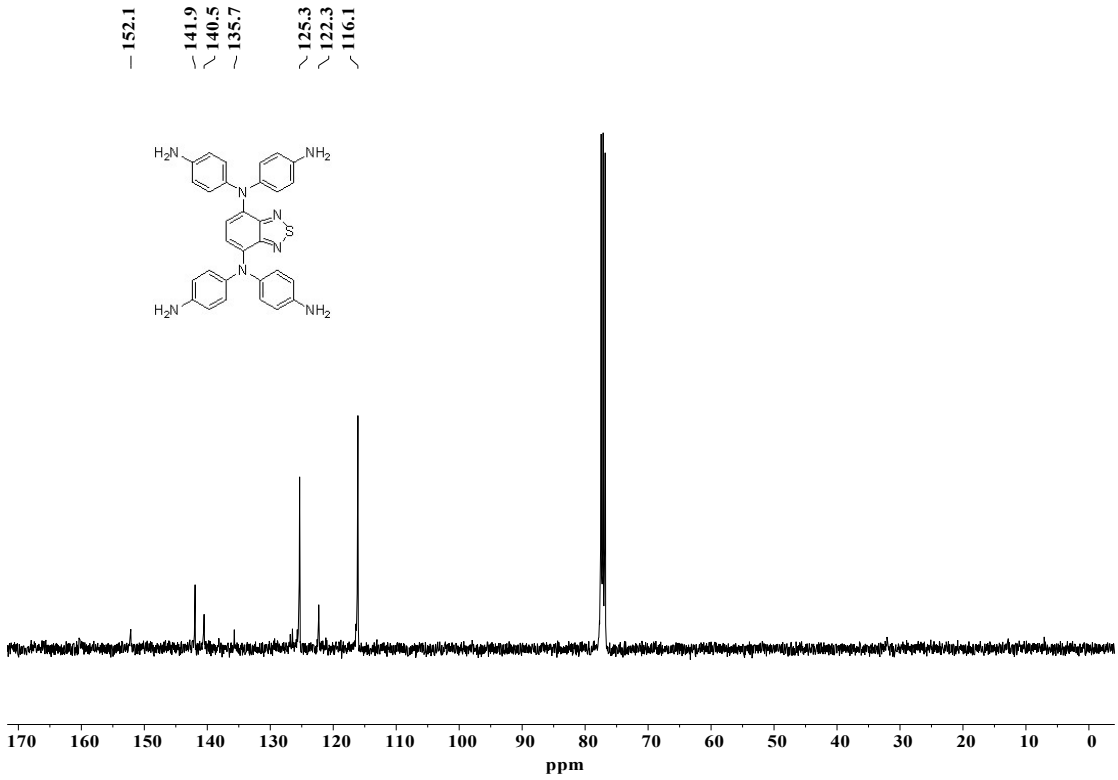

Figure S6. ^{13}C NMR spectrum of compound N^{1},N^{1}'-(benzo[*c*][1,2,5]thiadiazole-4,7-diyl)bis(N^{1}-(4-aminophenyl)benzene-1,4-diamine) (BTAPA) in $CDCl_3$.

Synthesis of HIAM-0022

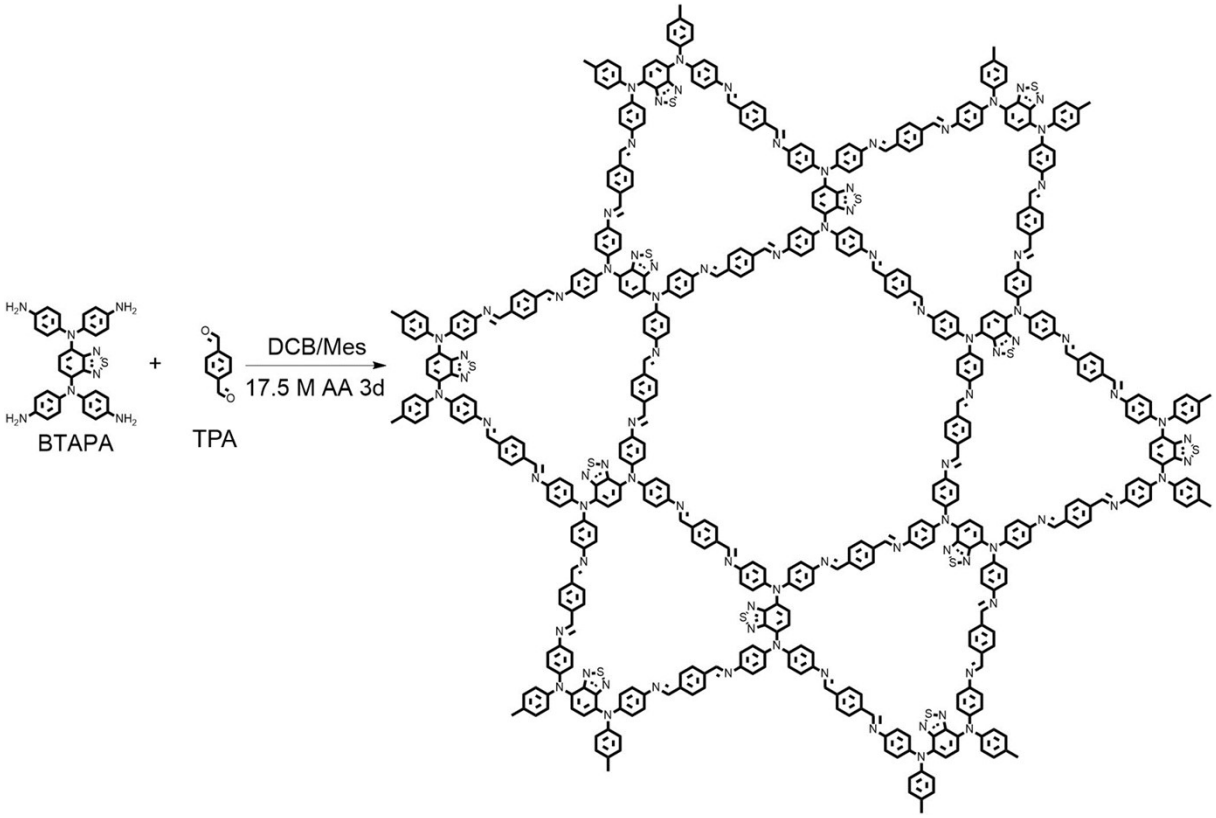

A Pyrex tube (10 mL) containing BTAPA (26 mg, 0.05 mmol), TPA (26 mg, 0.2 mmol), *o*-dichlorobenzene (*o*-DCB, 0.5 mL) and mesitylene (0.5 mL) was sonicated for 10 min. Then 17.5 M aqueous acetic acid (0.4 mL) was added to the above mixture solution. The tube was degassed through three freeze-pump-thaw cycles and then with kept at 120 °C for 72 h. After cooling to room temperature, the precipitate was collected by filtration and washed with THF for several times. Then the black solid was Soxhlet extracted in THF for 24 h and dried under 120 °C vacuum to afford HIAM-0022.

Synthesis of HIAM - 0023

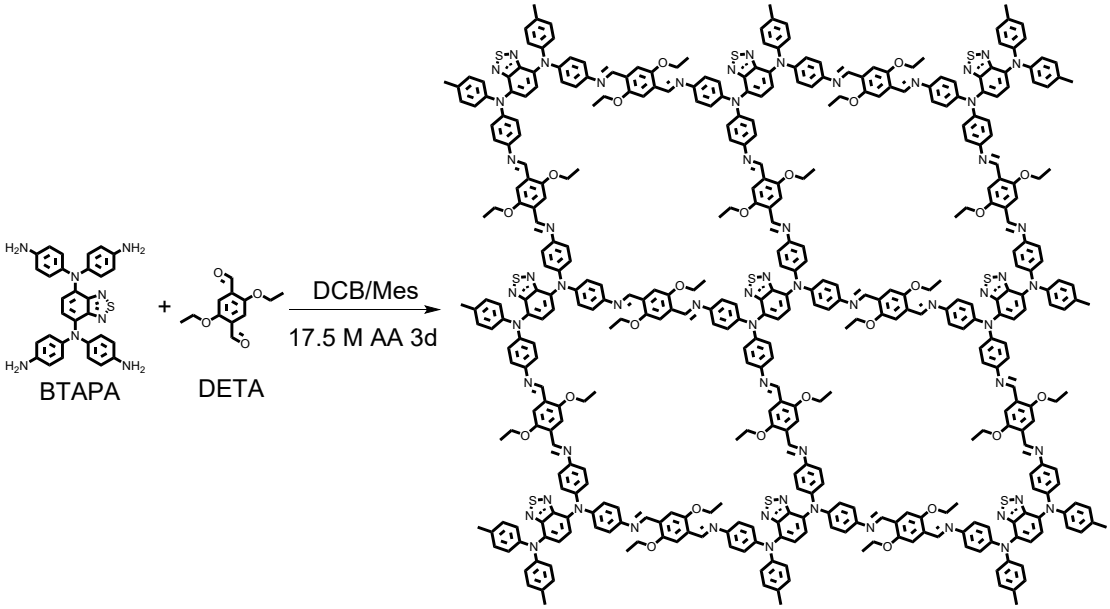

A Pyrex tube (10 mL) containing BTAPA (21 mg, 0.04 mmol), DETA (35 mg, 0.16 mmol), *o*-dichlorobenzene (*o*-DCB, 0.5 mL) and mesitylene (0.5 mL) was sonicated for 10 min. Then 17.5 M aqueous acetic acid (0.4 mL) was added to the above mixture solution. The tube was degassed through three freeze-pump-thaw cycles and then with kept at 120 °C for 72 h. After cooling to room temperature, the precipitate was collected by filtration and washed with THF for several times. Then the black solid was Soxhlet extracted in THF for 24 h and dried under 120 °C vacuum to afford HIAM-0023.

Synthesis of HIAM-0024

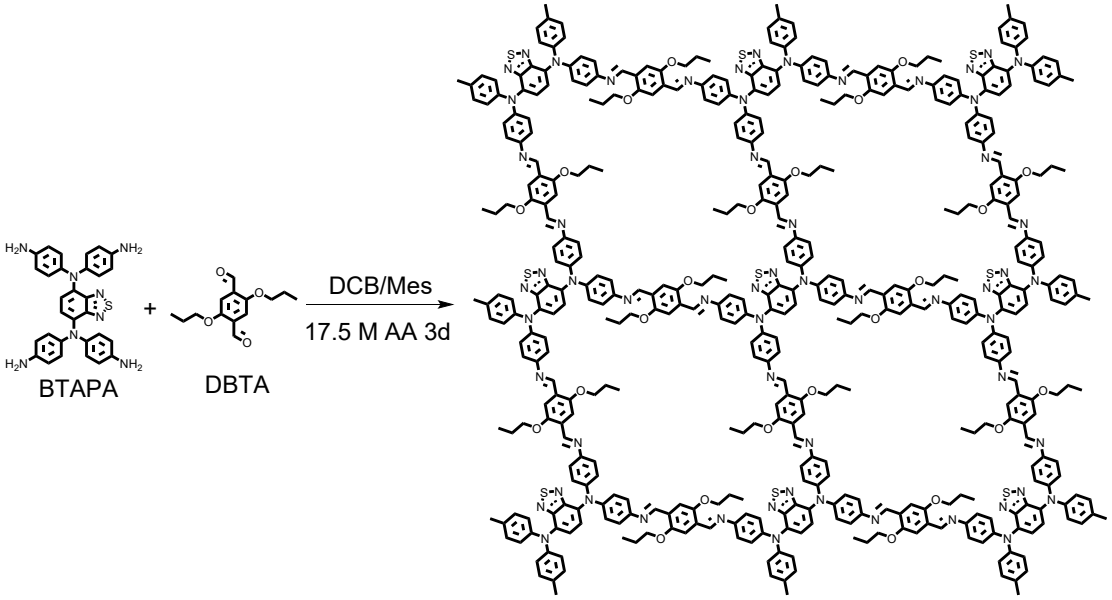

A Pyrex tube (10 mL) containing BTAPA (21 mg, 0.04 mmol), DBTA (40 mg, 0.16 mmol), *o*-dichlorobenzene (*o*-DCB, 0.5 mL) and mesitylene (0.5 mL) was sonicated for 10 min. Then 17.5 M aqueous acetic acid (0.4 mL) was added to the above mixture solution. The tube was degassed through three freeze-pump-thaw cycles and then with kept at 120 °C for 72 h. After cooling to room temperature, the precipitate was collected by filtration and washed with THF for several times. Then the black solid was Soxhlet extracted in THF for 24 h and dried under 120 °C vacuum to afford HIAM-0024.

Synthesis of HIAM-0025

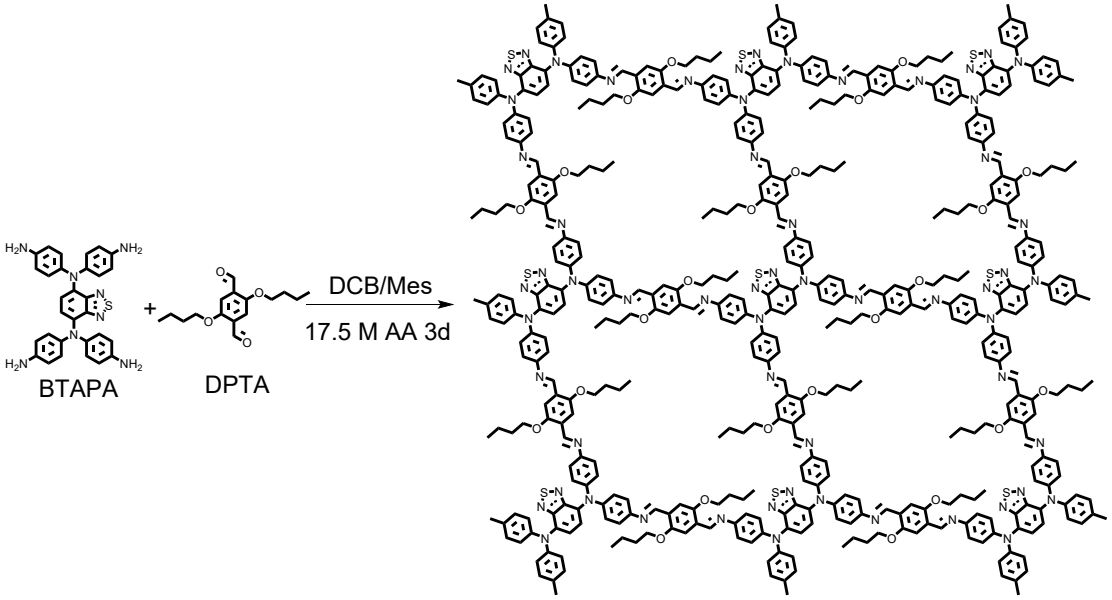

A Pyrex tube (10 mL) containing BTAPA (21 mg, 0.04 mmol), DPTA (44 mg, 0.16 mmol), *o*-dichlorobenzene (*o*-DCB, 0.5 mL) and mesitylene (0.5 mL) was sonicated for 10 min. Then 17.5 M aqueous acetic acid (0.4 mL) was added to the above mixture solution. The tube was degassed through three freeze-pump-thaw cycles and then with kept at 120 °C for 72 h. After cooling to room temperature, the precipitate was collected by filtration and washed with THF for several times. Then the black solid was Soxhlet extracted in THF for 24 h and dried under 120 °C vacuum to afford HIAM-0025.

Synthesis of HIAM-0023-X% (X = 12.5, 25, 37.5, 50)

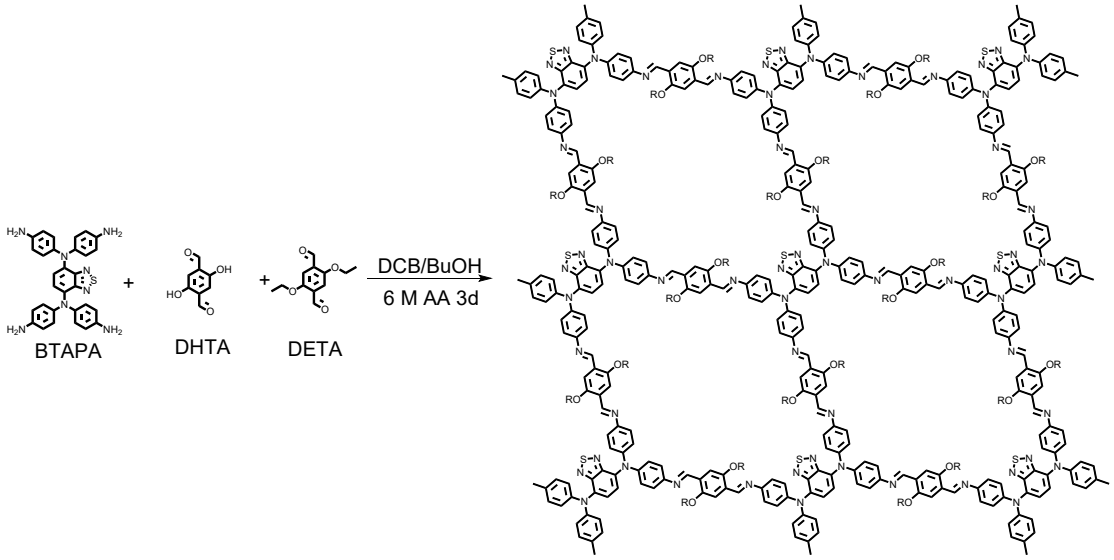

A Pyrex tube (10 mL) containing BTAPA (21 mg, 0.04 mmol), DHTA (1.7 mg, 0.01 mmol), DETA (16 mg, 0.07 mmol), *o*-dichlorobenzene (*o*-DCB, 1.5 mL) and *n*-butanol (0.5 mL) was sonicated for 10 min. Then 6 M aqueous acetic acid (0.2 mL) was added to the above mixture solution. The tube was degassed through three freeze-pump-thaw cycles and then with kept at 120 °C for 72 h. After cooling to room temperature, the precipitate was collected by filtration and washed with THF for several times. Then the black solid was Soxhlet extracted in THF for 24 h and dried under 120 °C vacuum to afford HIAM-0023-12.5%.

Other three COFs were also prepared through the similar procedure only by varying the precursor amount of DHTA and DETA.

HIAM-0023-25% : 3.3 mg, 0.02 mmol DHTA and 13 mg, 0.06 mmol DETA.

HIAM-0023-37.5% : 5 mg, 0.03 mmol DHTA and 11 mg, 0.05 mmol DETA.

HIAM-0023-50% : 6.4 mg, 0.04 mmol DHTA and 9 mg, 0.04 mmol DETA.

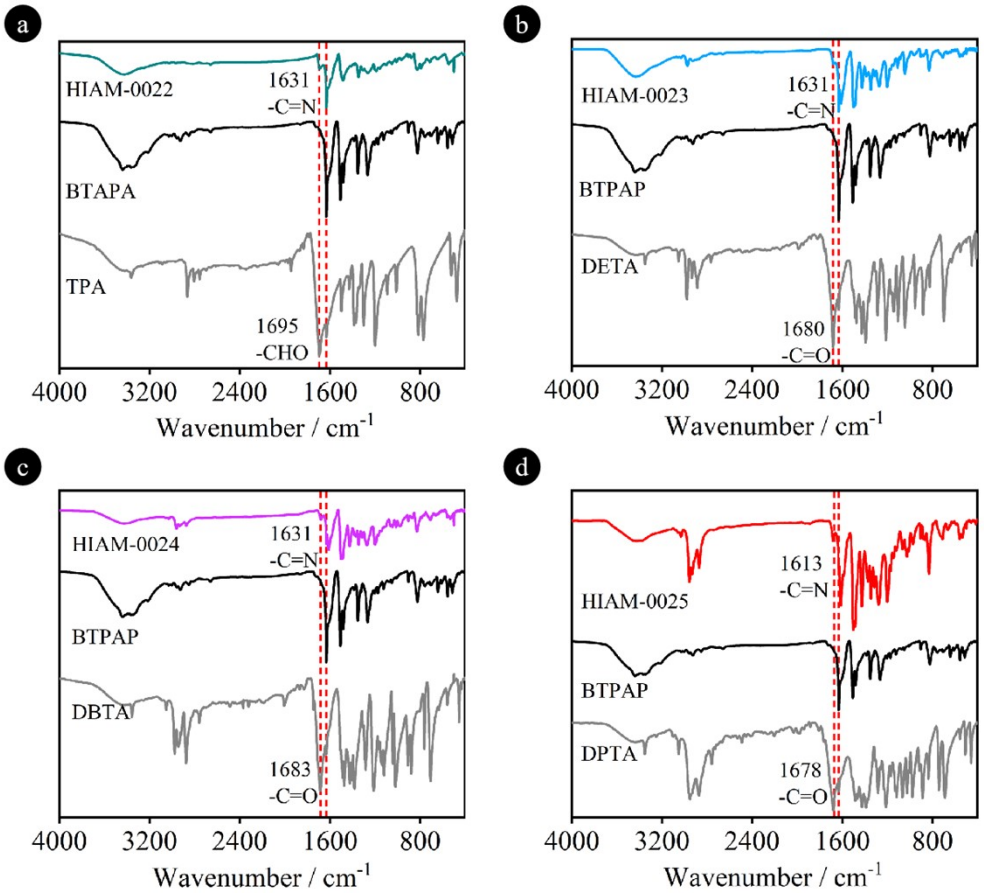

Figure S7. The FT-IR spectra of (a) HIAM-0022, (b) HIAM-0023, (c) HIAM-0024 and (d) HIAM-0025 and the corresponding organic building units.

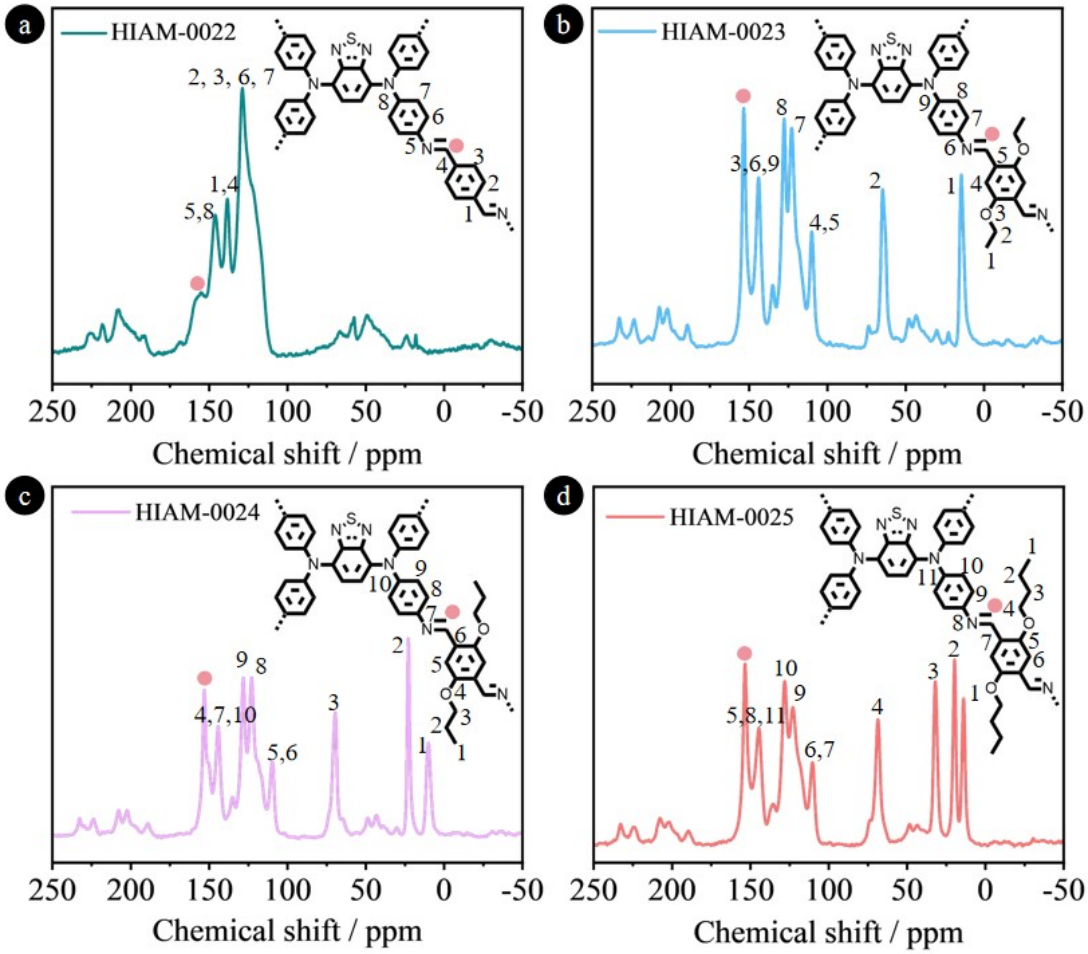

Figure S8. Solid-state ^{13}C NMR spectra of (a) HIAM-0022, (b) HIAM-0023, (c) HIAM-0024 and (d) HIAM-0025.

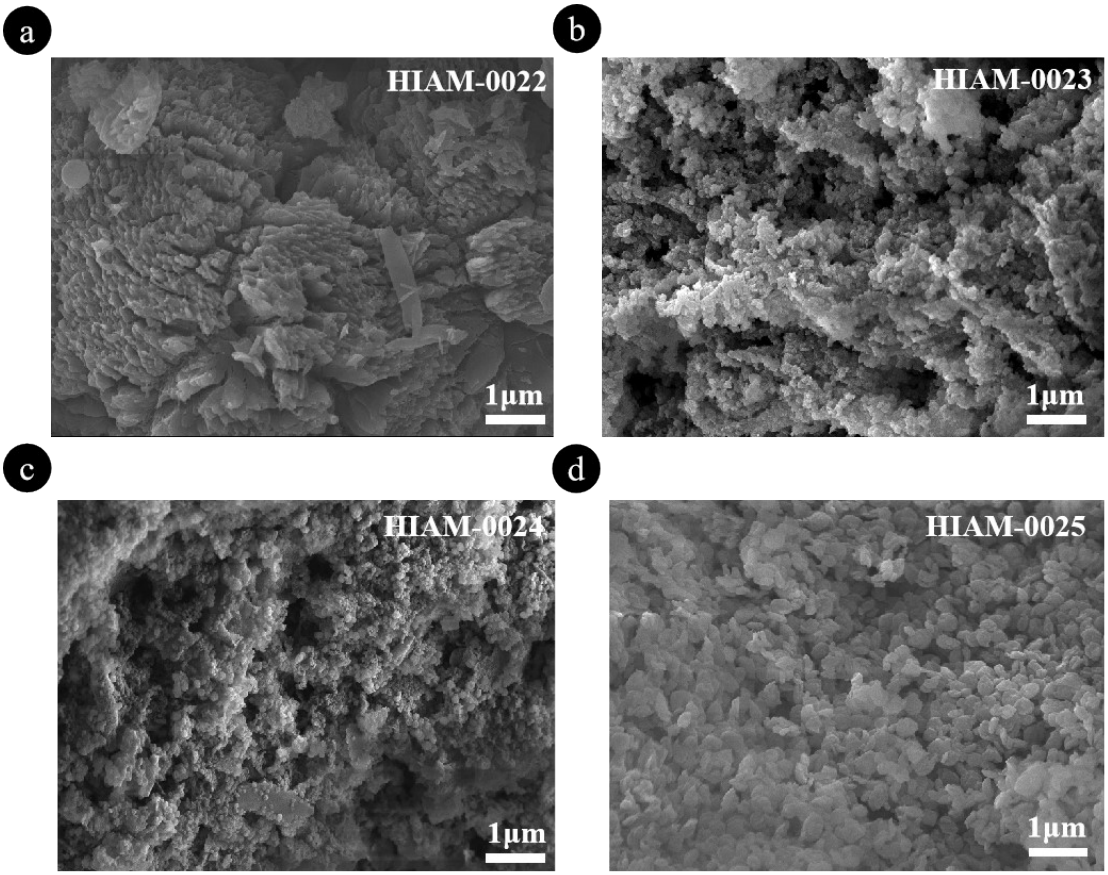

Figure S9. SEM images of (a) HIAM-0022, (b) HIAM-0023, (c) HIAM-0024 and (5) HIAM-0025.

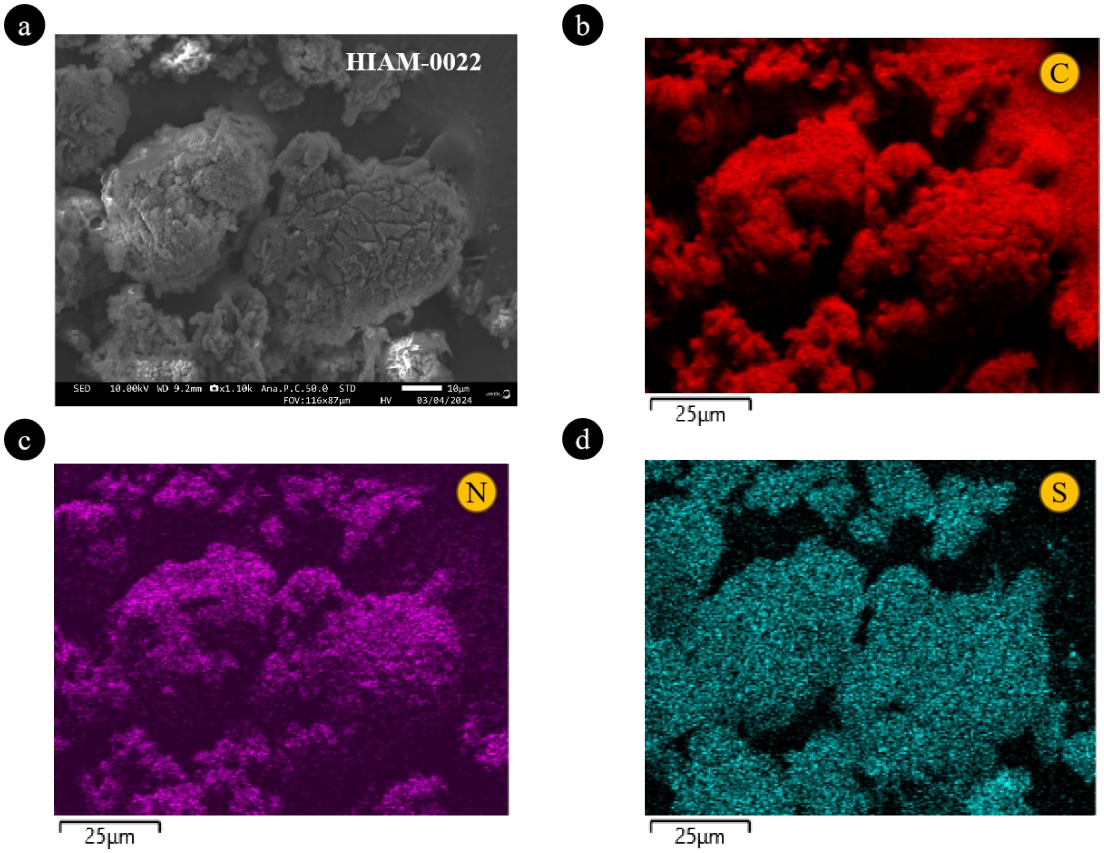

Figure S10. Energy dispersive X-ray analysis of HIAM-0022.

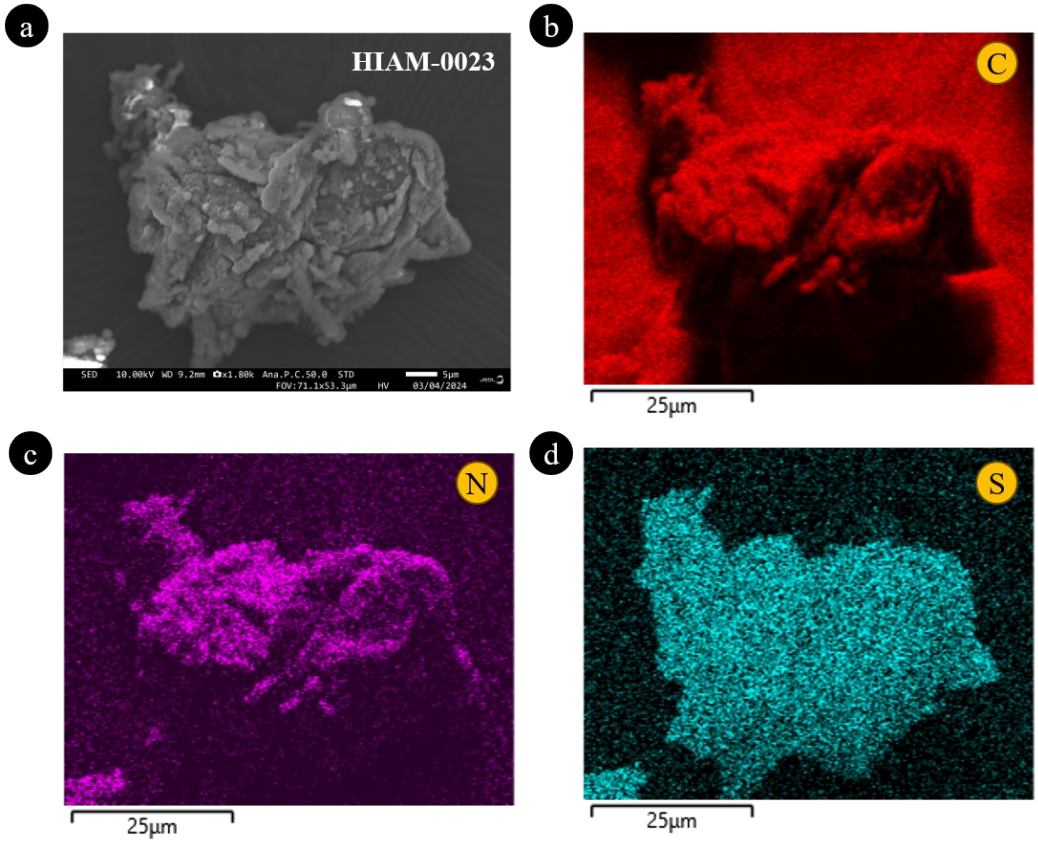

Figure S11. Energy dispersive X-ray analysis of HIAM-0023.

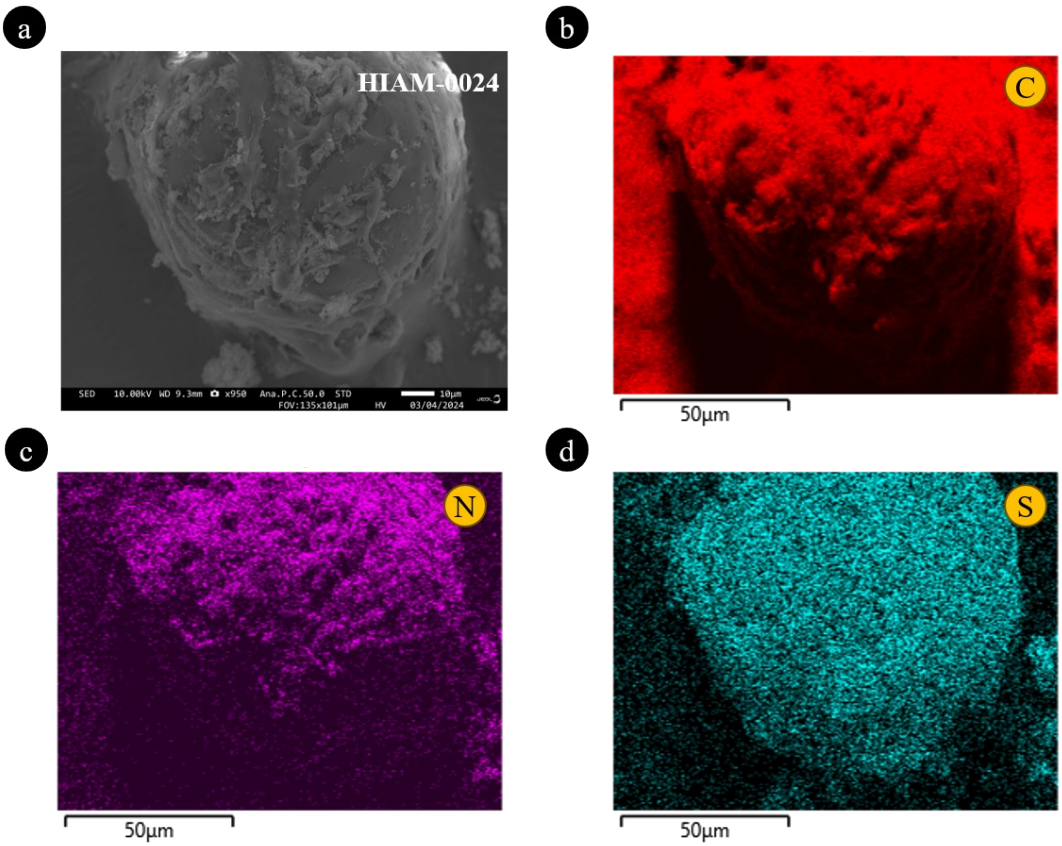

Figure S12. Energy dispersive X-ray analysis of HIAM-0024.

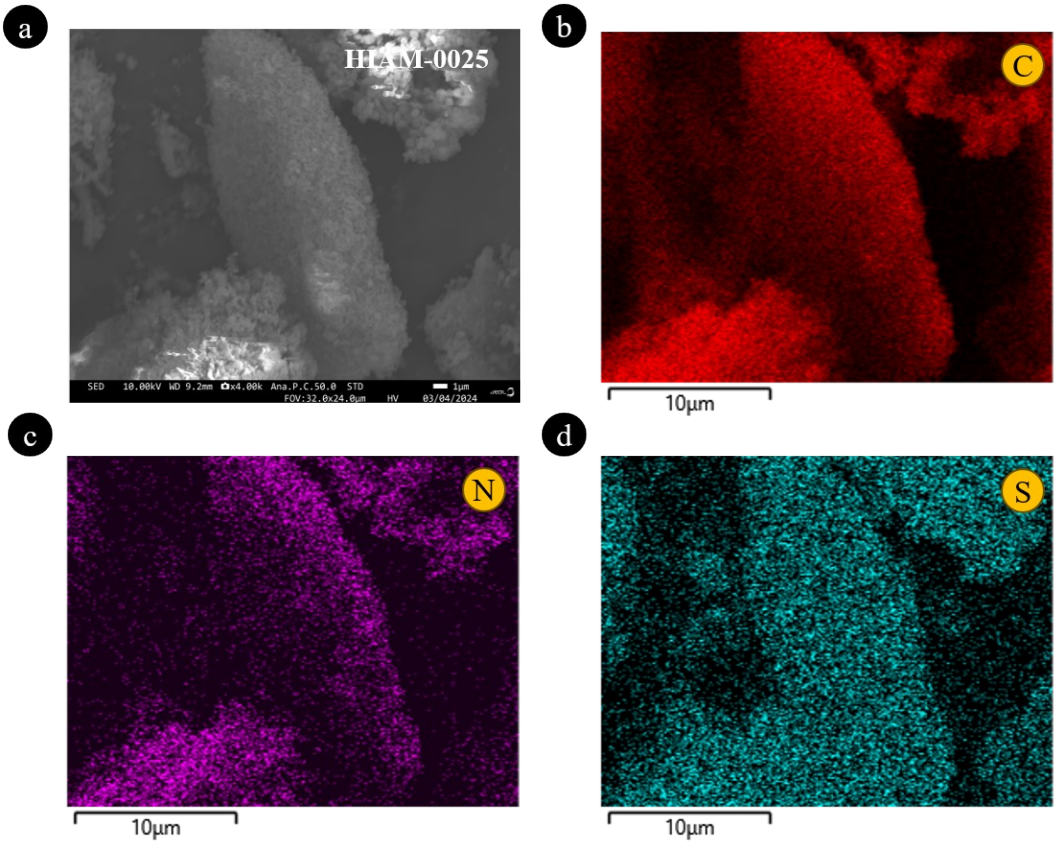

Figure S13. Energy dispersive X-ray analysis of HIAM-0025.

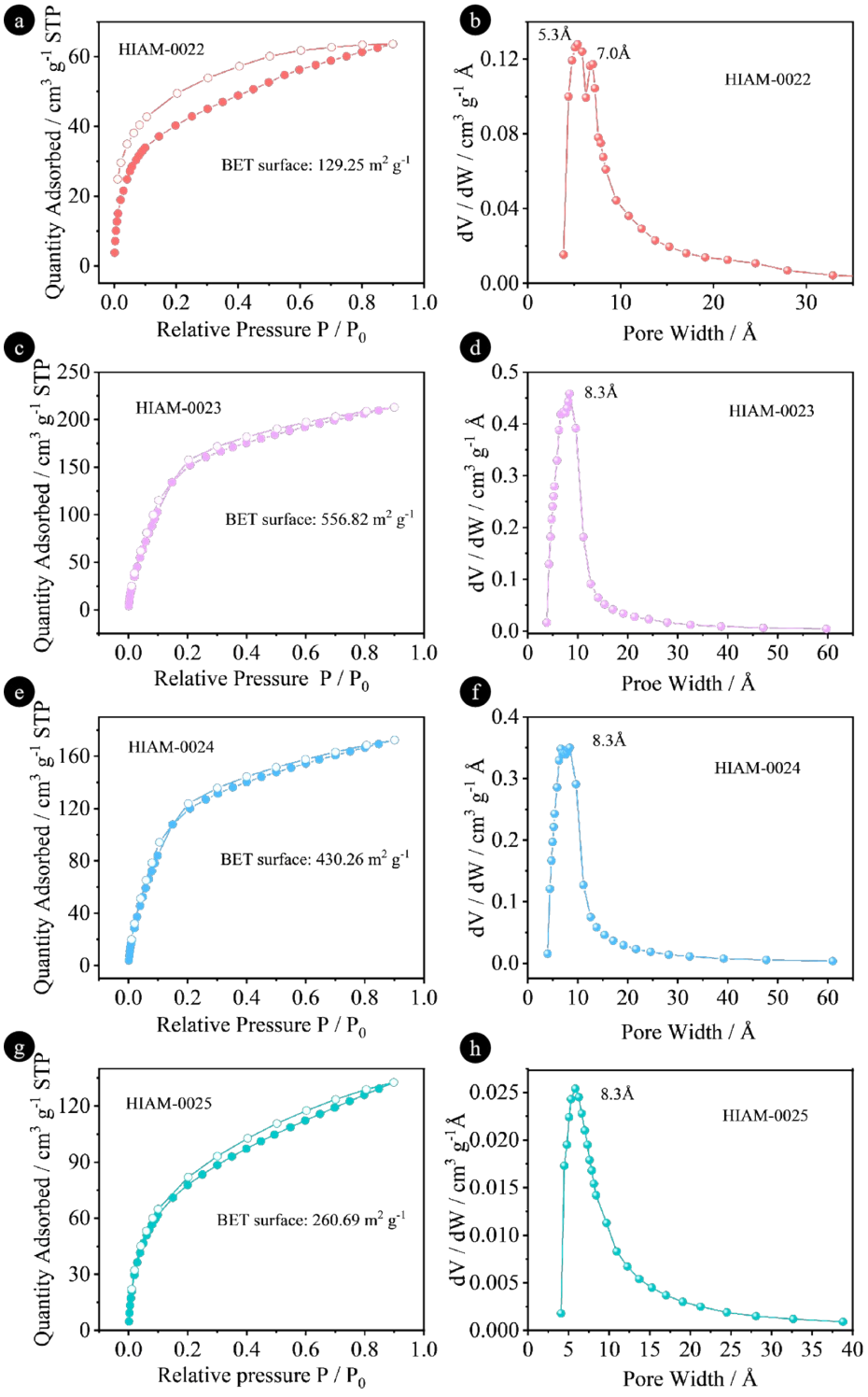

Figure S14. The CO_2 adsorption-desorption isotherms of (a) HIAM-0022, (c) HIAM-0023, (e) HIAM-0024 and (g) HIAM-0025. The calculated pore size distributions of (b) HIAM-0022, (d) HIAM-0023, (f) HIAM-0024 and (h) HIAM-0025.

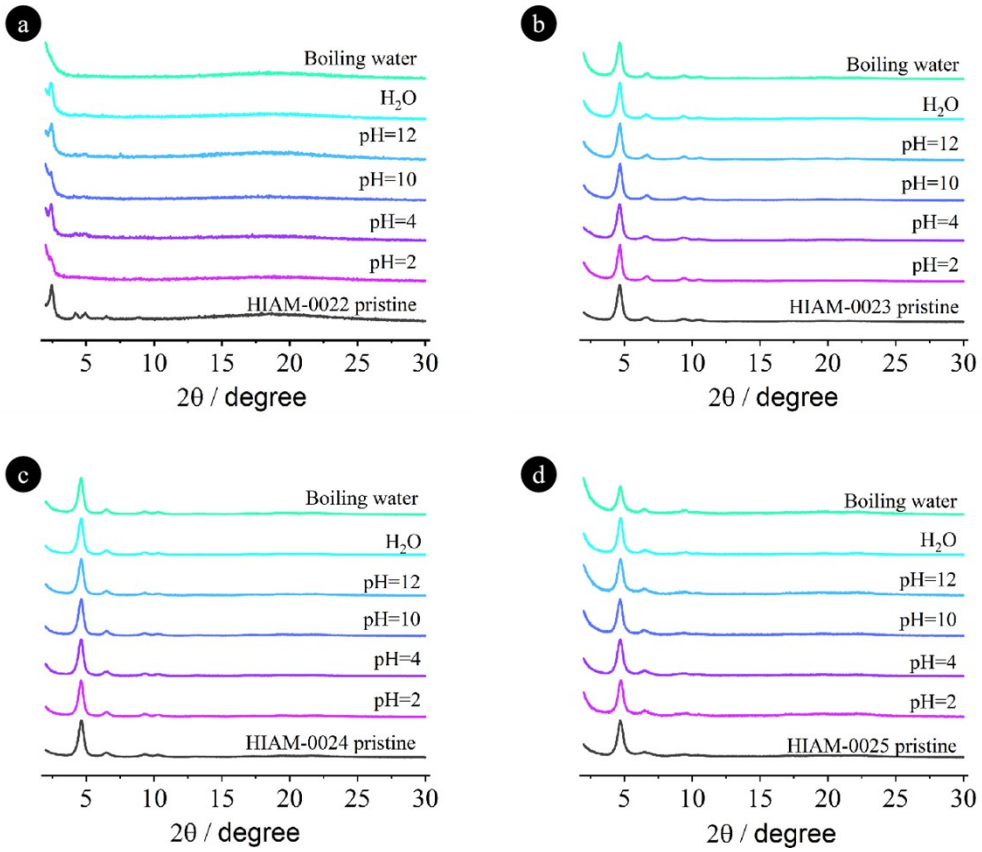

Figure S15. The PXRD patterns of (a) HIAM-0022, (b) HIAM-0023, (c) HIAM-0024 and (d) HIAM-0025 after treatment under various conditions for 24 hours.

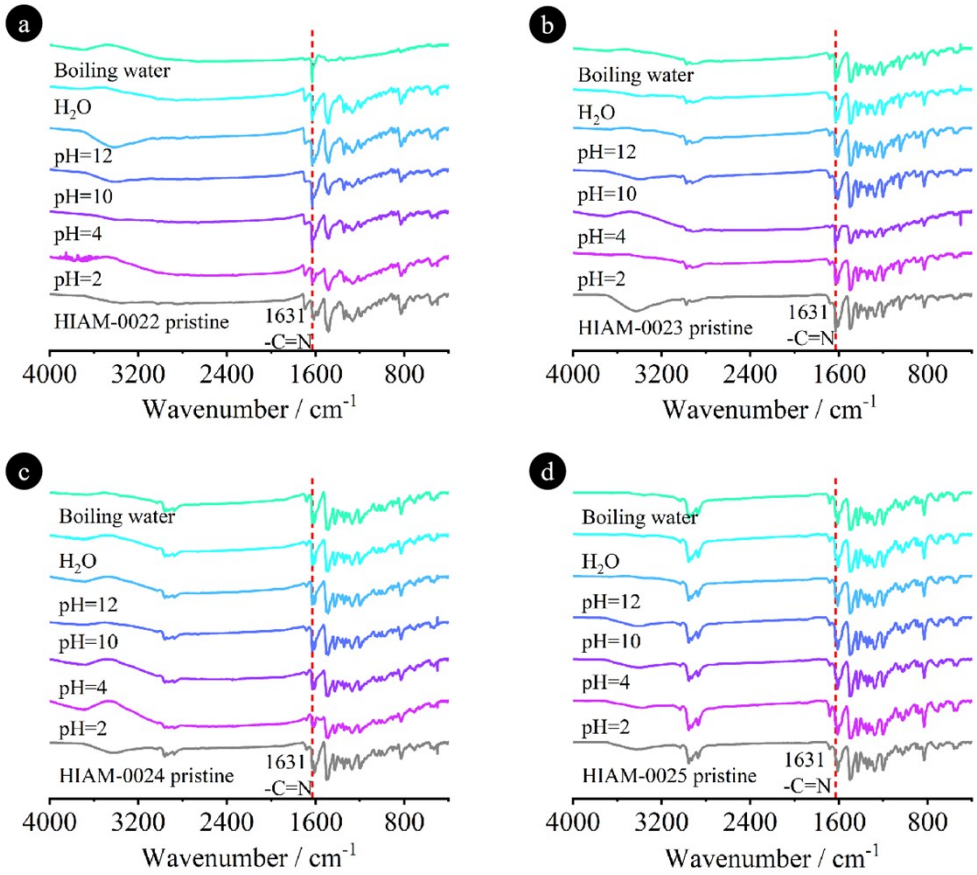

Figure S16. The FT-IR spectra of (a) HIAM-0022, (b) HIAM-0023, (c) HIAM-0024 and (d) HIAM-0025 after treatment under various conditions for 24 hours.

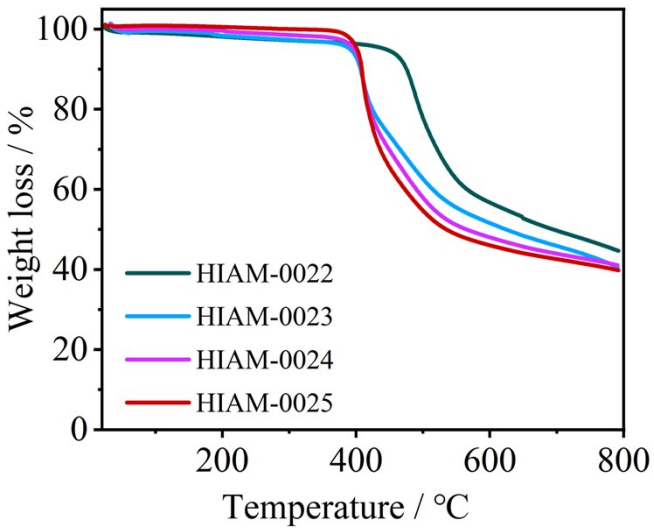

Figure S17. TGA curves of HIAM-0022, HIAM-0023, HIAM-0024 and HIAM-0025.

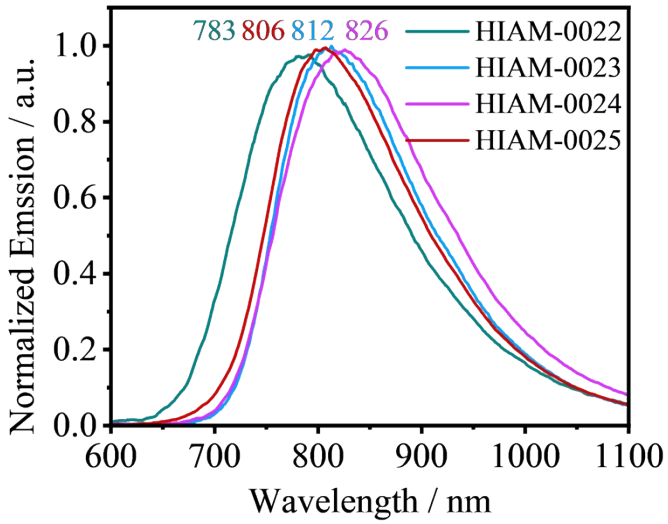

Figure S18. Normalized emission spectra of the HIAM-0022, HIAM-0023, HIAM-0024 and HIAM-0025.

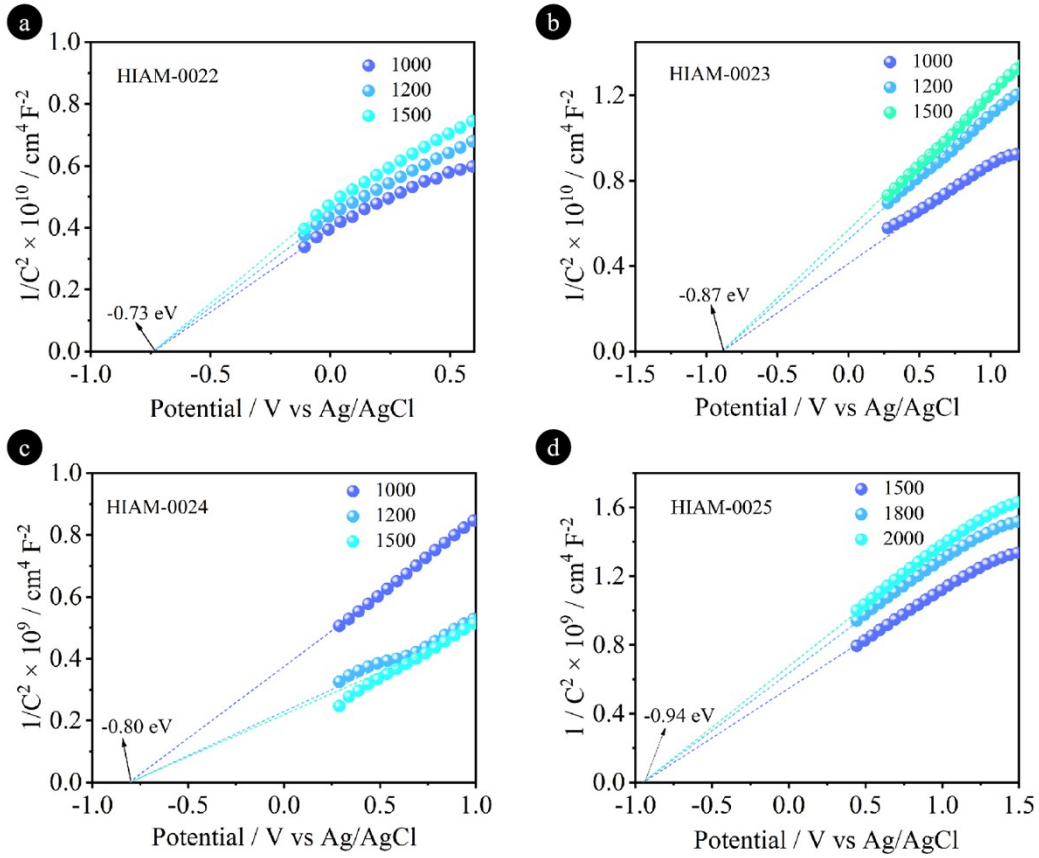

Figure S19. Mott-Schottky plots of (a) HIAM-0022, (b) HIAM-0023, (c) HIAM-0024 and (d) HIAM-0025.

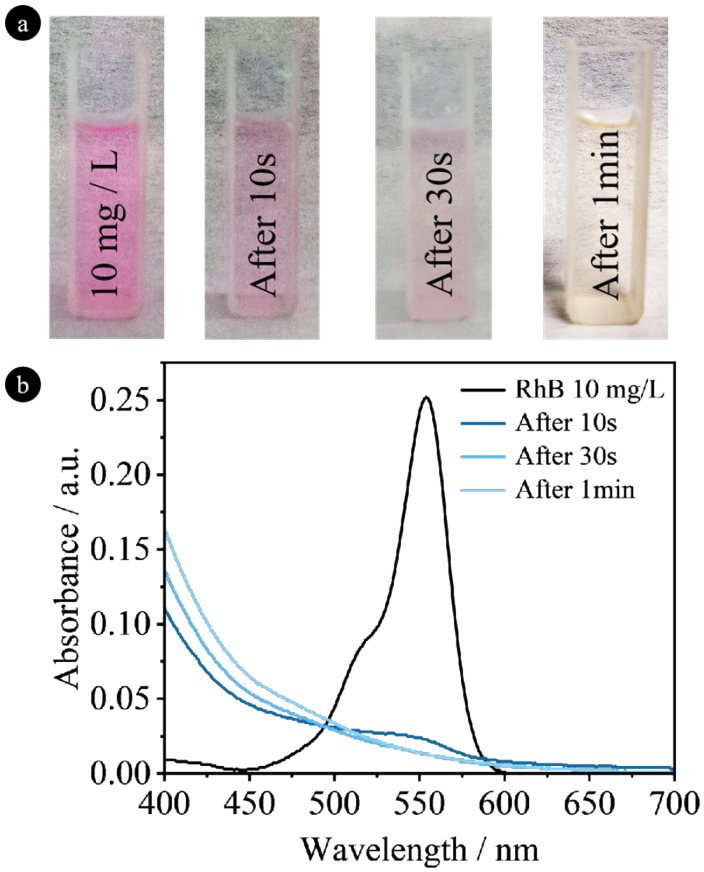

Figure S20. The RhB (10 mg L^{-1}) decomposition using produced H_2O_2 solution via a Fenton reaction: (a) Color change with time and (b) its corresponding absorbance. Detailed process: 10 mg of RhB and 278 mg of $FeSO_4 \cdot 7H_2O$ were dissolved in a 1 L of volumetric flask. Taking out 2 mL of RhB solution and put it in a 4 mL cuvette, and then 1 mL of photocatalytic H_2O_2 solution after a prolonged photocatalytic reaction (8 h) was added. The color change of RhB and absorbance were recorded at 10 s, 30 s and 1 min.

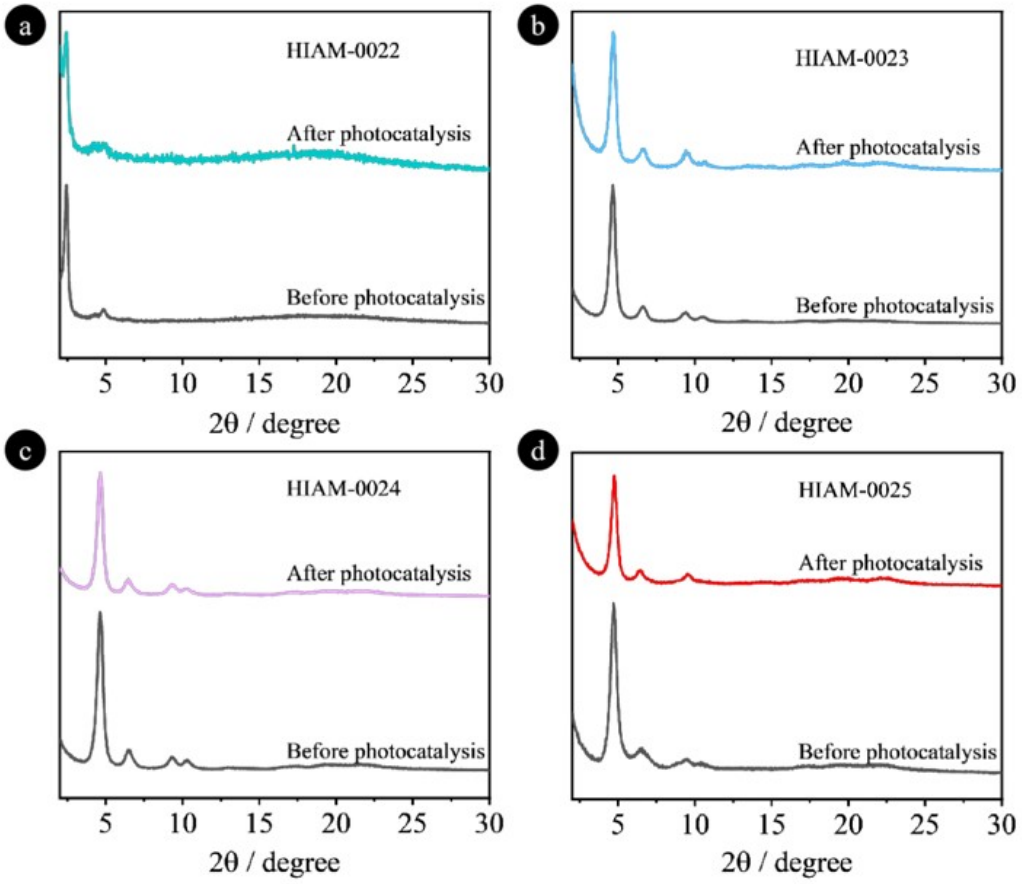

Figure S21. The PXRD patterns of (a) HIAM-0022, (b) HIAM-0023, (c) HIAM-0024 and (d) HIAM-0025 before and after photocatalytic measurement.

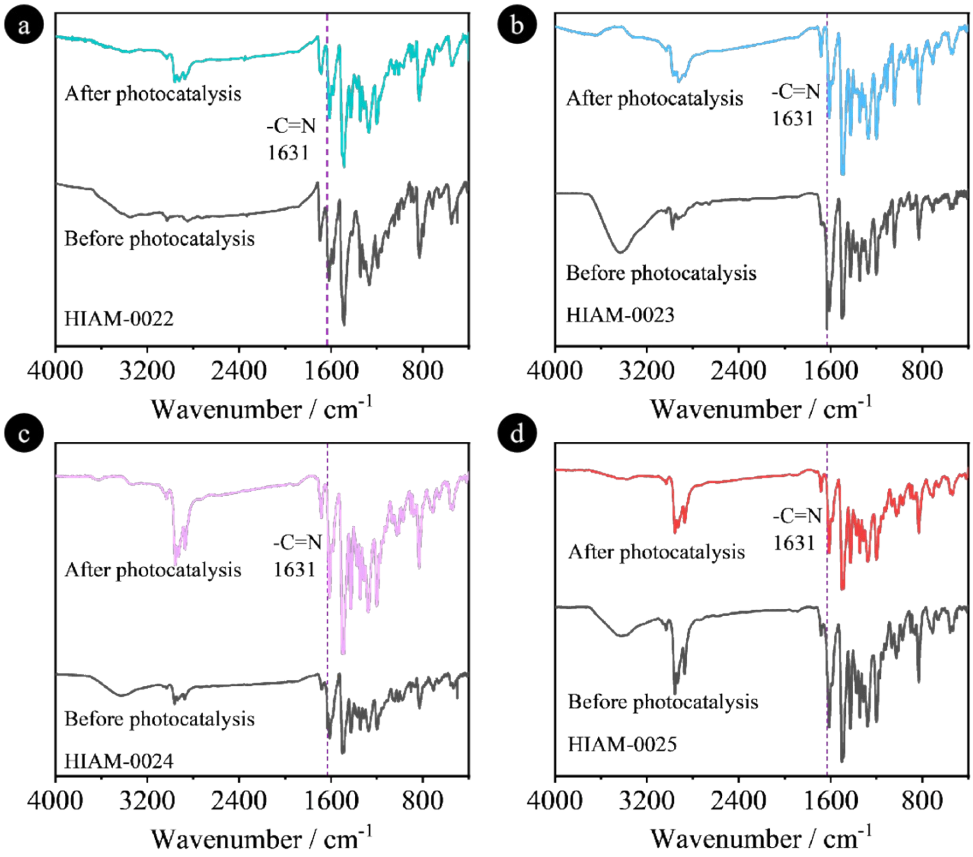

Figure S22. The FT-IR spectra of (a) HIAM-0022, (b) HIAM-0023, (c) HIAM-0024 and (d) HIAM-0025 before and after photocatalytic measurement.

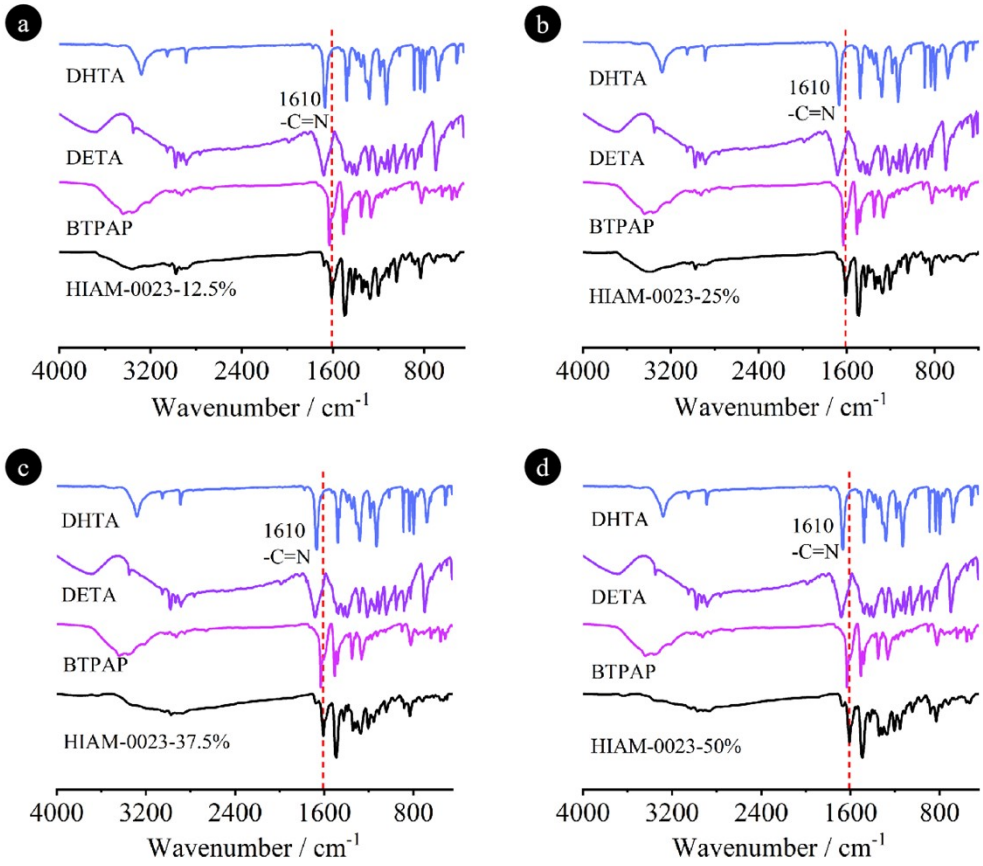

Figure S23. The FT-IR spectra of (a) HIAM-0023-12.5%, (b) HIAM-0023-25%, (c) HIAM-0023-37.5% and (d) HIAM-0023-50% and the corresponding organic building units.

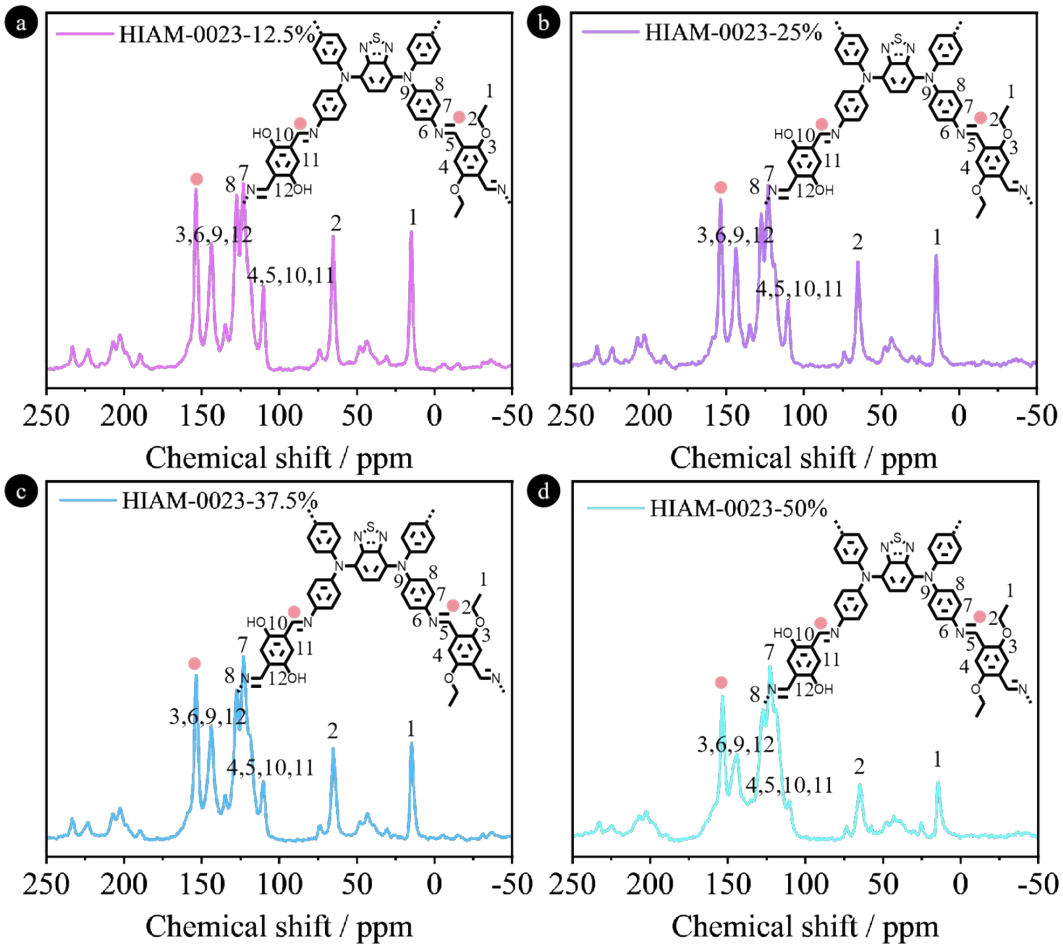

Figure S24. Solid-state ^{13}C NMR spectra of (a) HIAM-0023-12.5%, (b) HIAM-0023-25%, (c) HIAM-0023-37.5% and (d) HIAM-0023-50%.

Table S1. Summary of synthesis of HIAM-0023-X% series, their stoichiometric linker input ratio and the output ratio observed in their compounds.

COF	BTAPA Stoichiometry / mmol	DHTA+DETA Stoichiometry / mmol	DHTA:DETA Stoichiometric ratio	DHTA:DETA ratio observed
HIAM-0023-12.5%	0.04	0.08	1:7	1:6.4
HIAM-0023-25%	0.04	0.08	1:3	1:2.06
HIAM-0023-37.5%	0.04	0.08	1:1.6	1:1.19
HIAM-0023-50%	0.04	0.08	1:1	1:0.42

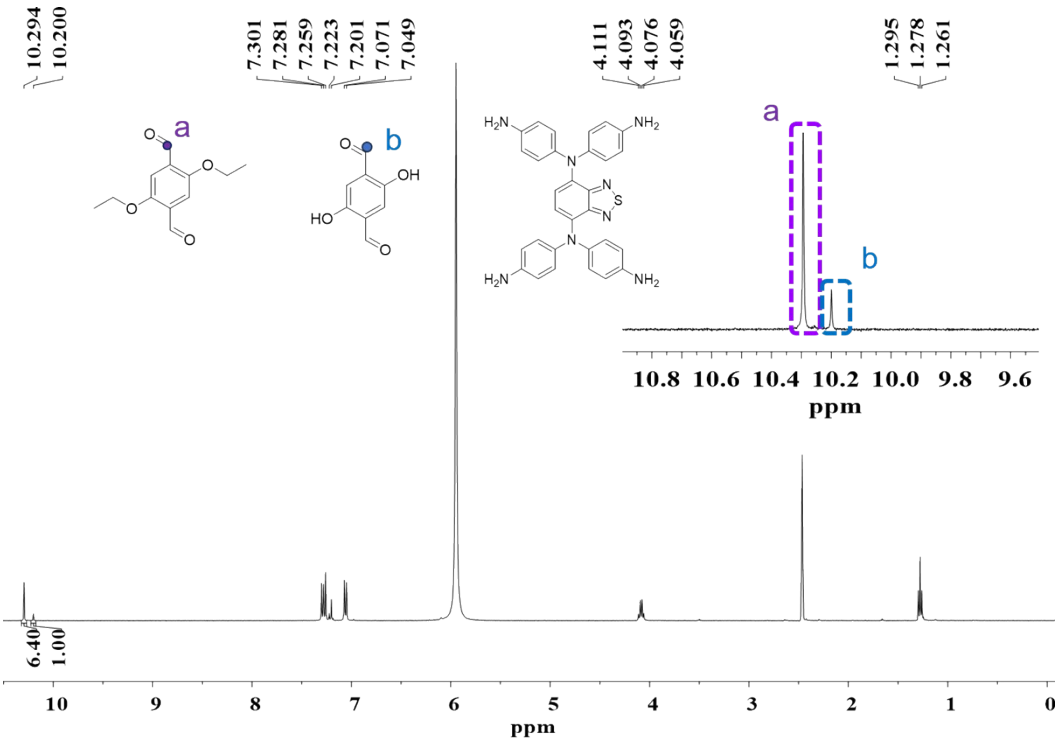

Figure S25. ^{1}H NMR spectrum of the digested HIAM-0023-12.5%. The peak region between 9.6 to 10.8 ppm has been magnified in the inset.

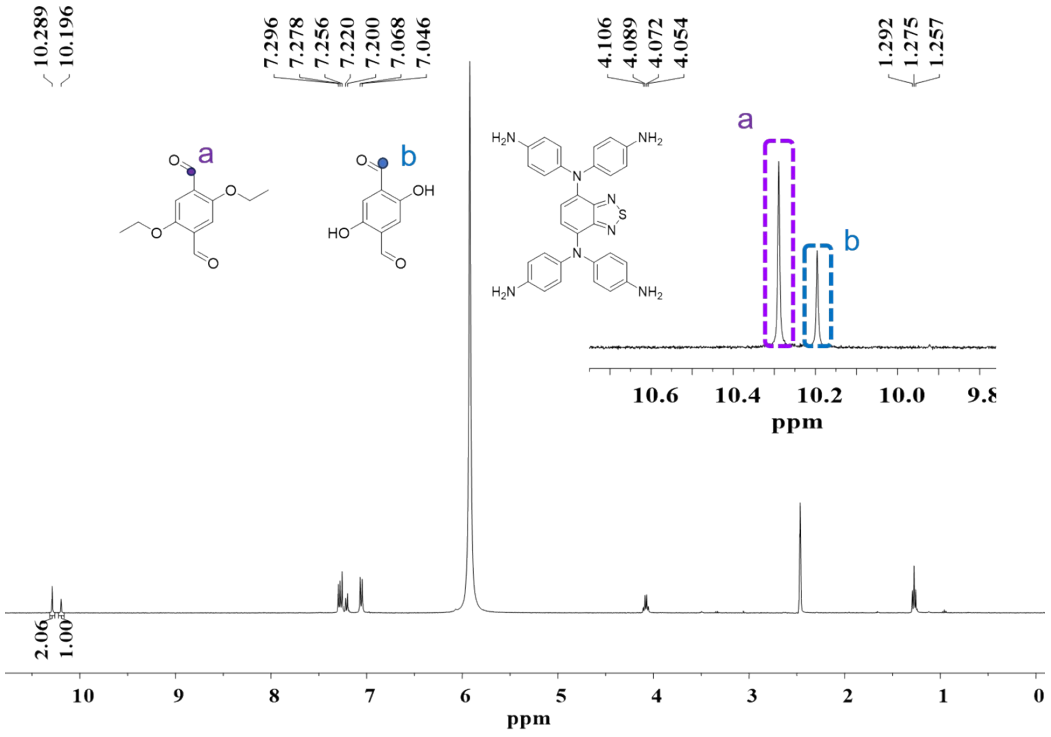

Figure S26. ^{1}H NMR spectrum of the digested HIAM-0023-25%. The peak region between 9.6 to 10.8 ppm has been magnified in the inset.

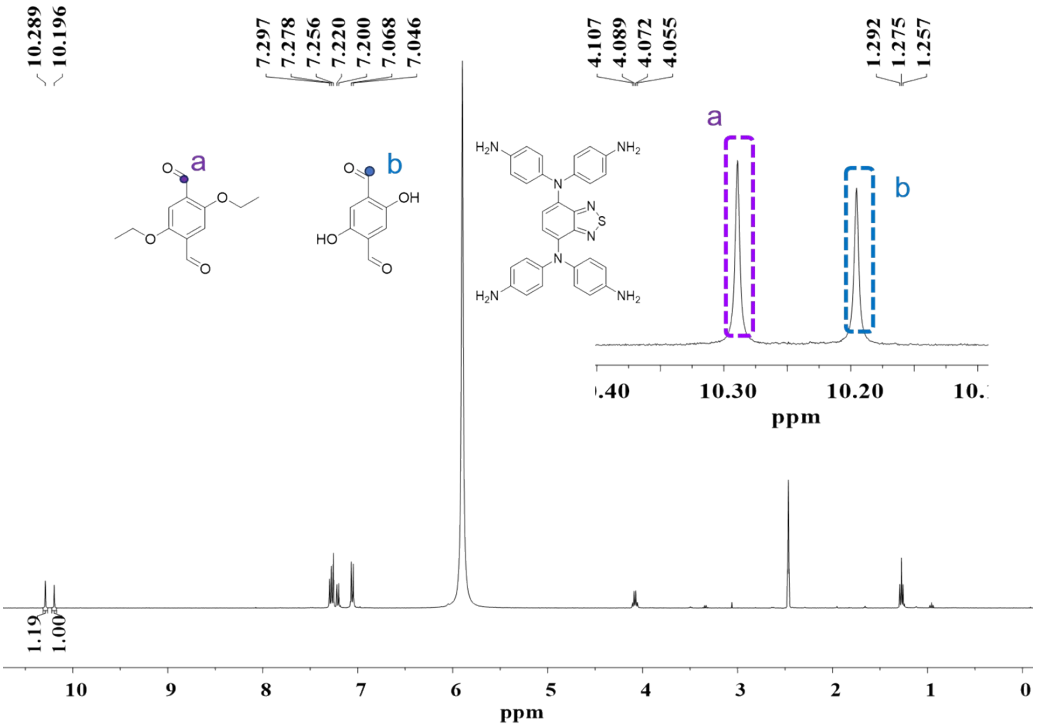

Figure S27. [1]H NMR spectrum of the digested HIAM-0023-37.5%. The peak region between 9.6 to 10.8 ppm has been magnified in the inset.

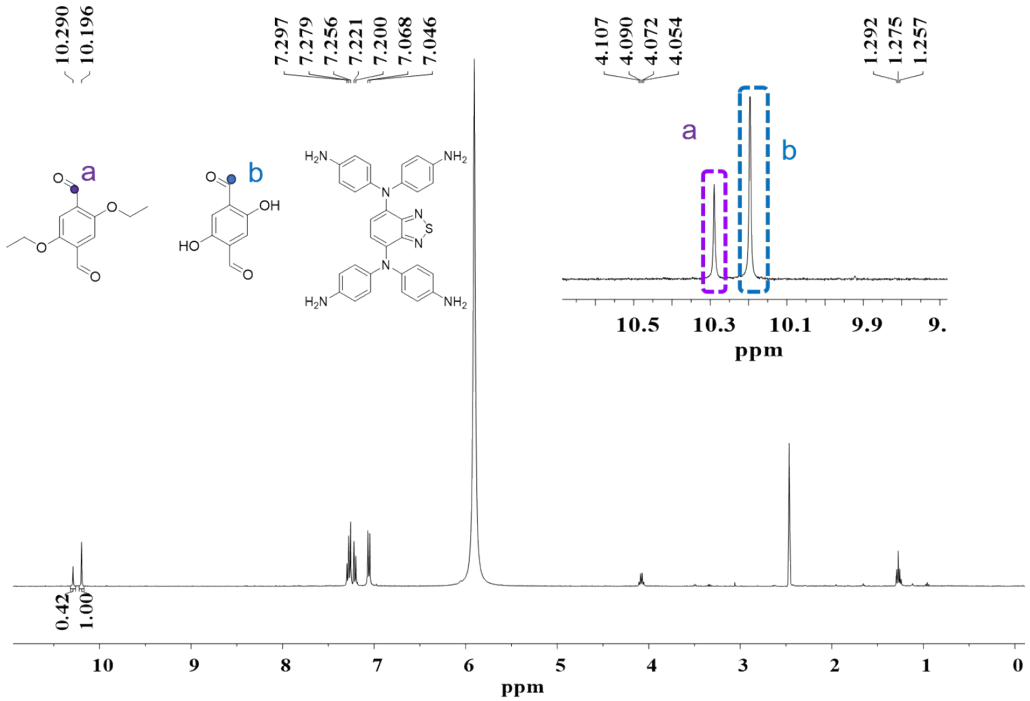

Figure S28. [1]H NMR spectrum of the digested HIAM-0023-50%. The peak region between 9.6 to 10.8 ppm has been magnified in the inset.

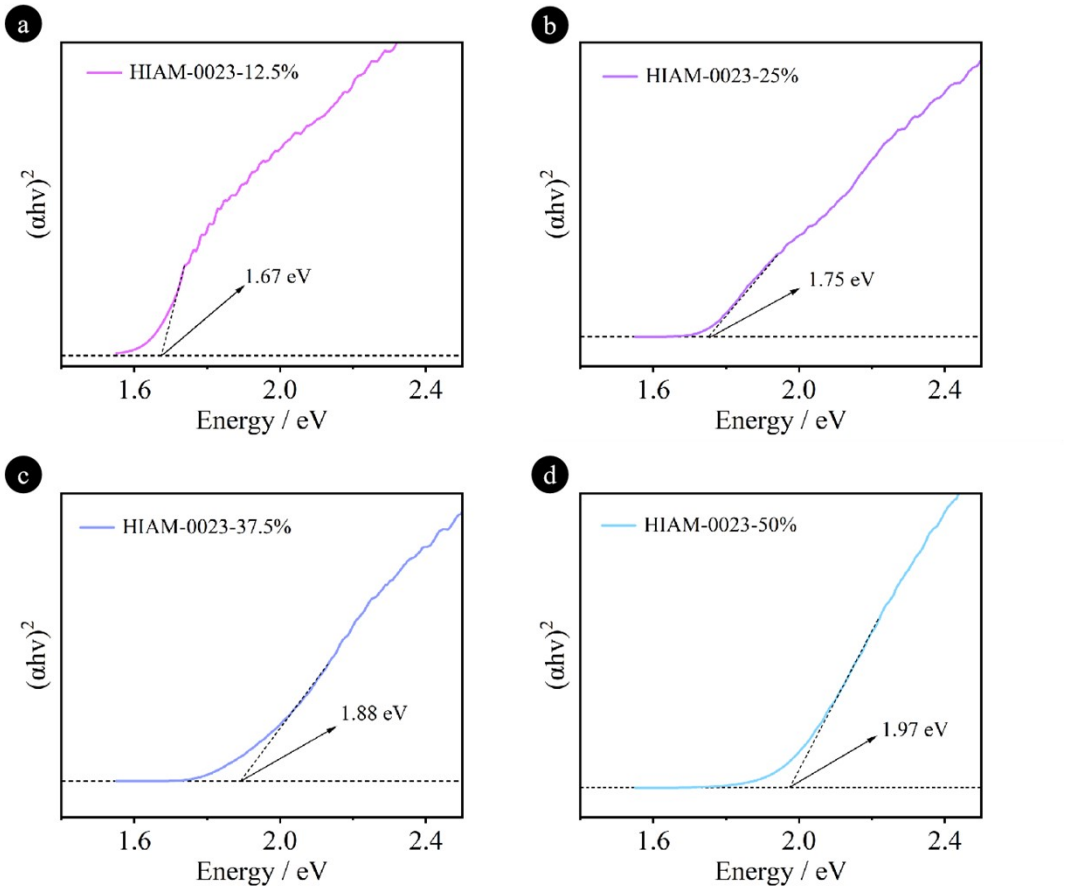

Figure S29. The Tauc plot of (a) HIAM-0023-12.5%, (b) HIAM-0023-25%, (c) HIAM-0023-37.5% and (d) HIAM-0023-50%.

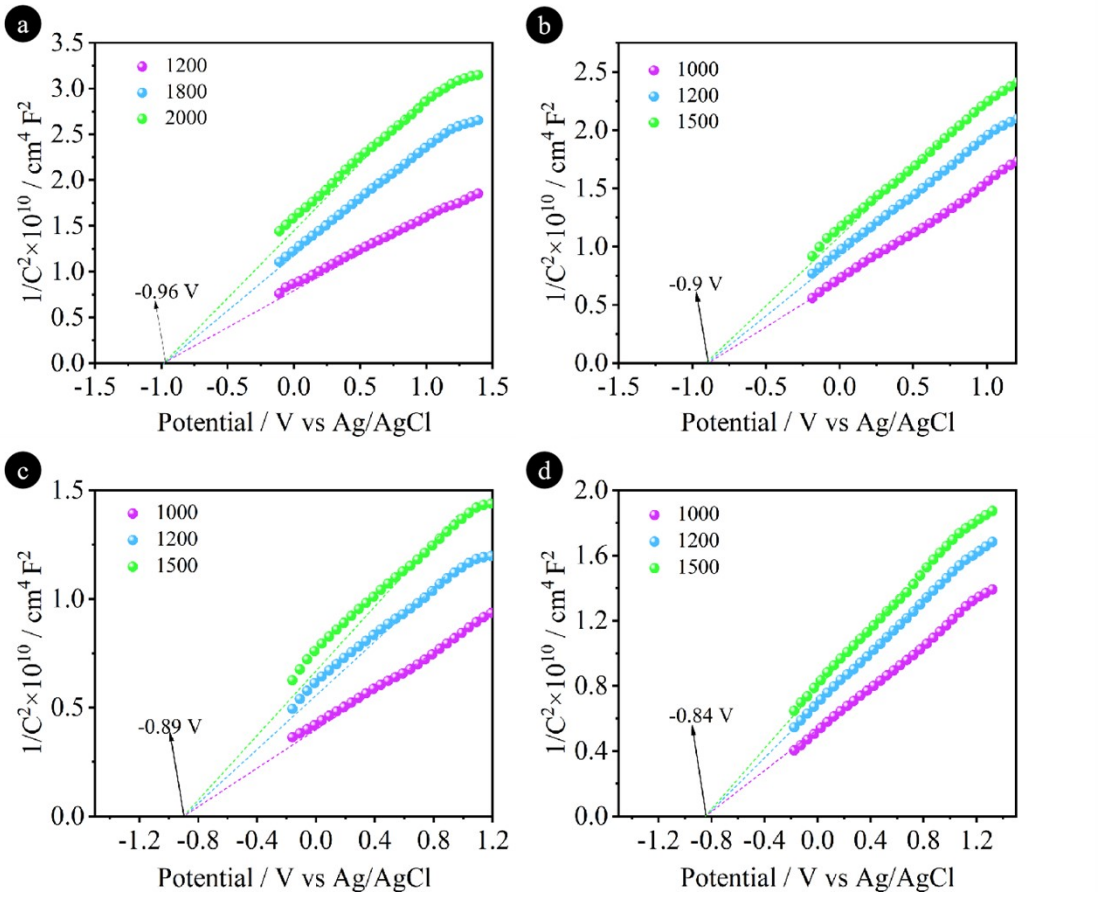

Figure S30. Mott-Schottky plots of (a) HIAM-0023-12.5%, (b) HIAM-0023-25%, (c) HIAM-0023-37.5% and (d)HIAM-0023-50%.

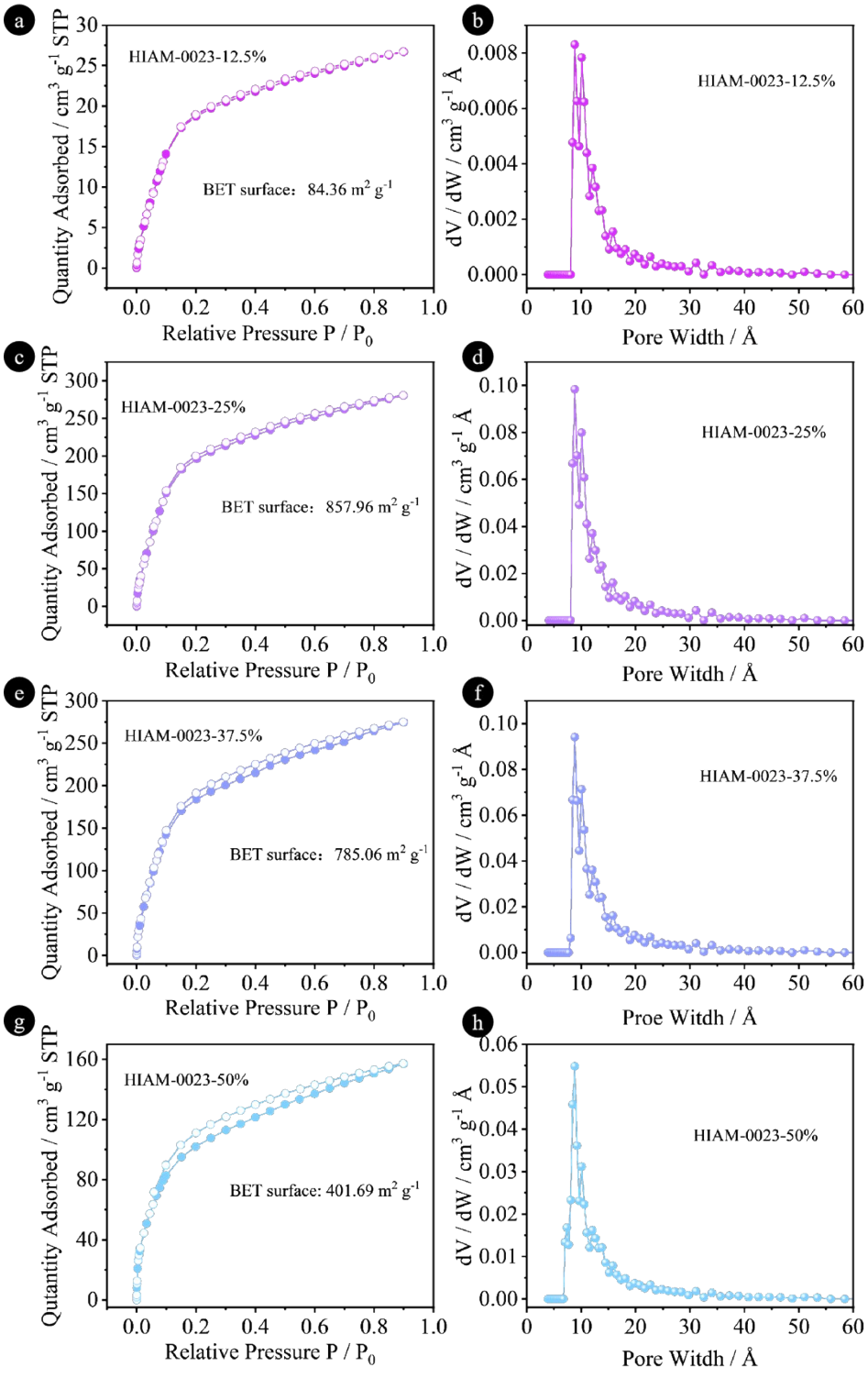

Figure S31. The CO_2 adsorption-desorption isotherms of (a) HIAM-0023-12.5%, (c) HIAM-0023-25%, (e) HIAM-0023-37.5% and (g) HIAM-0023-50%. The calculated pore size distributions of (b) HIAM-0023-12.5%, (d) HIAM-0023-25%, (f) HIAM-0023-37.5% and (h) HIAM-0023-50%.

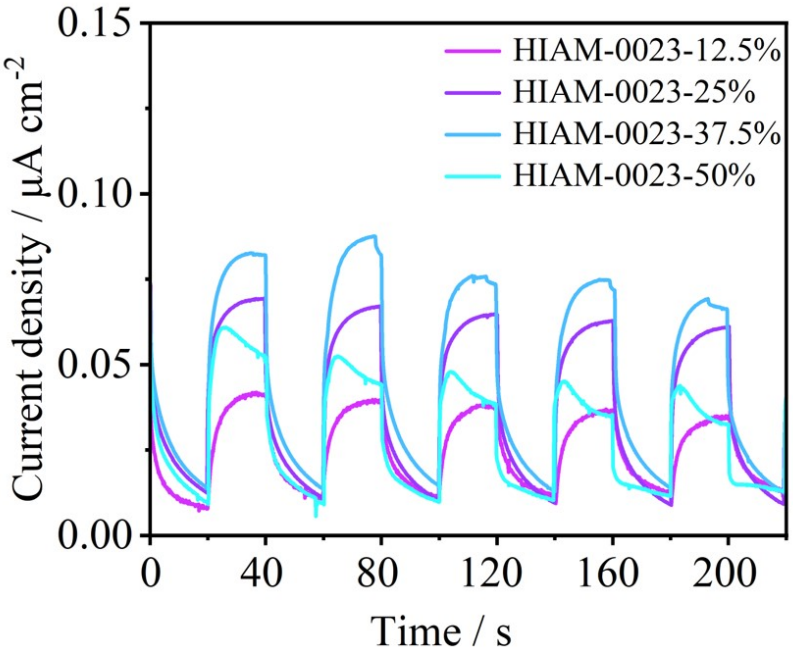

Figure S32. Transient photocurrent of the HIAM-0023-X% (X = 12.5, 25, 37.5 and 50) under λ > 420 nm.

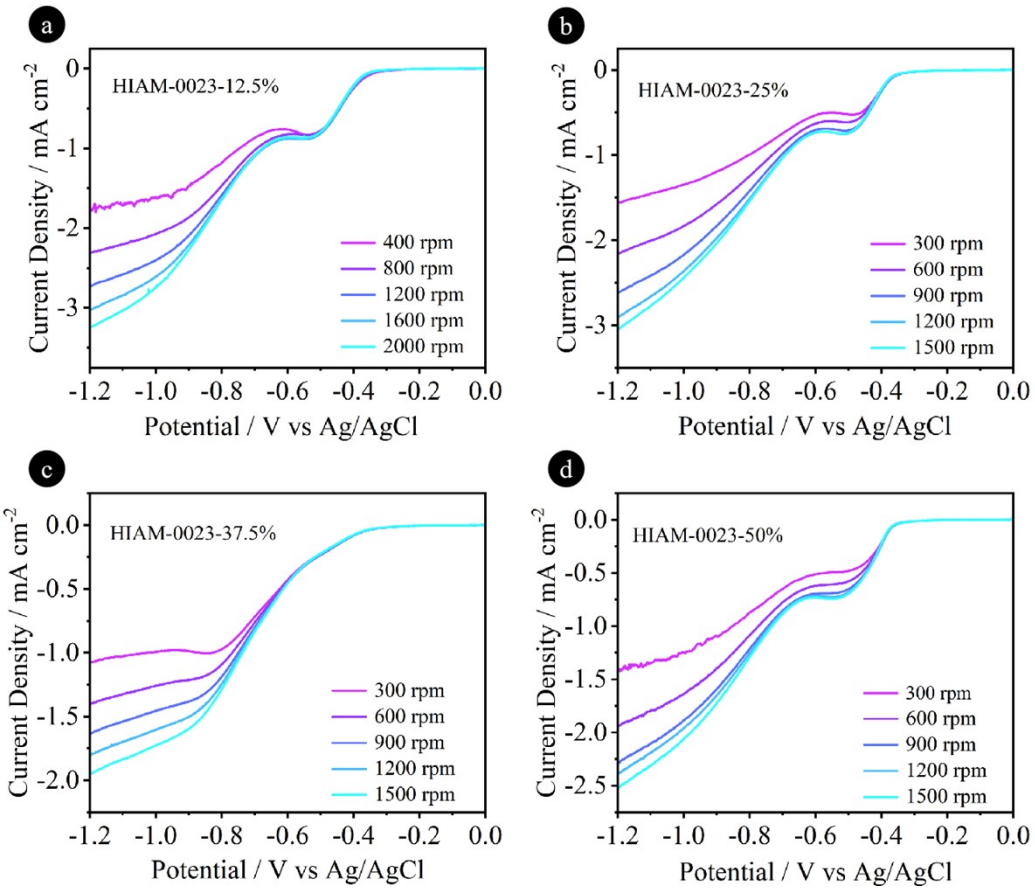

Figure S33. Linear-sweep RDE voltammograms of (a) HIAM-0023-12.5%, (b) HIAM-0023-25%, (c) HIAM-0023-37.5% and (d) HIAM-0023-50% measured at different rotating speeds.

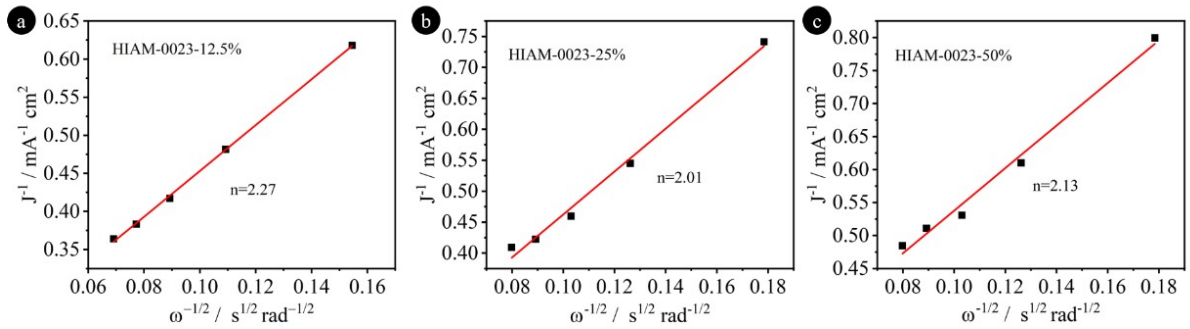

Figure S34. Kouteckly-Levich plots obtained by RDE tests in phosphate buffer (pH = 7) solution of (a) HIAM-0023-12.5%, (b) HIAM-0023-25% and (c) HIAM-0023-50%.

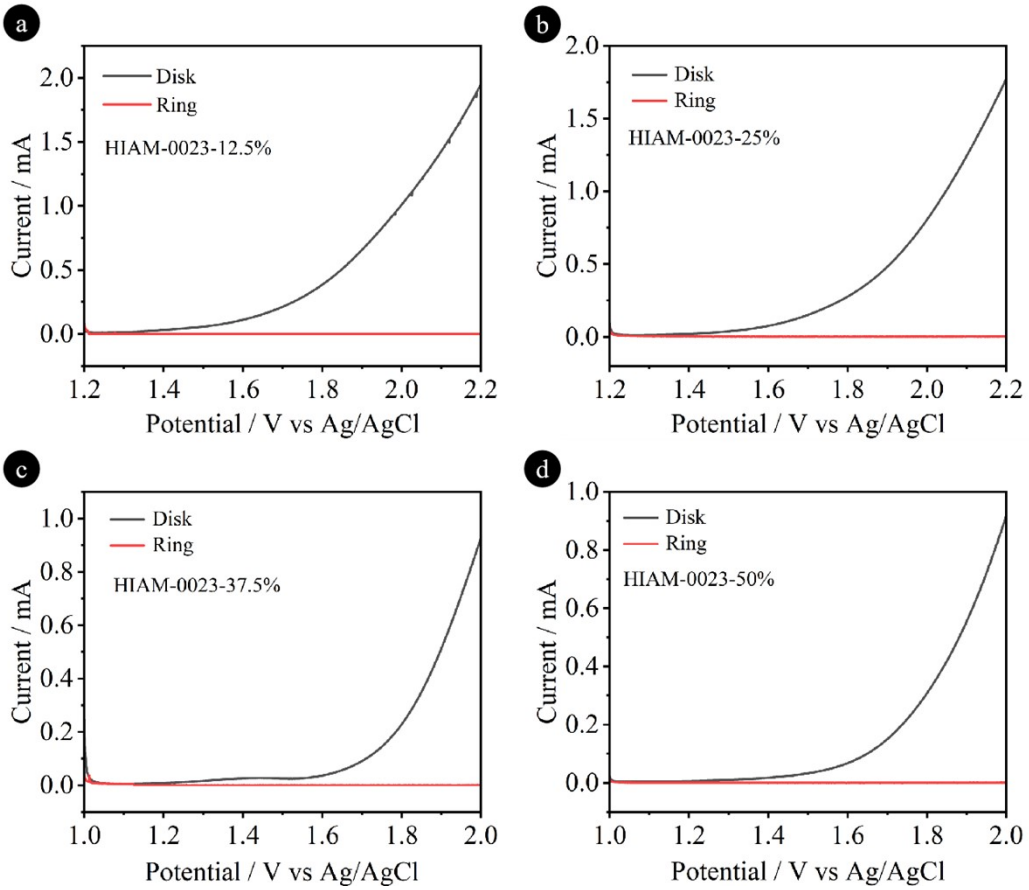

Figure S35. Rotating ring-disk electrode voltammograms of (a) HIAM-0023-12.5%, (b) HIAM-0023-25%, (c) HIAM-0023-37.5% and (d) HIAM-0023-50% obtained in 0.1 M phosphate buffer solution (pH = 7) with a scan rate of 10 mV s^{-1} and a rotation rate of 1600 rpm. The potential of Pt ring electrode was set at 0.6 V versus Ag/AgCl to detect H_2O_2.

Table S2. Unit cell parameters and fractional atomic coordinates for HIAM-0022 based on the AA-stacking.

Space group	PM		
Calculated unit cell	a = c = 43.6752 Å, b = 3.4977 Å α = γ = 90°, β = 59.1945°		
C1	0.31982	-0.00000	0.16436
C2	0.35016	-0.00000	0.16697
C3	0.34695	-0.00000	0.20068
C4	0.31329	-0.00000	0.23183
C5	0.28303	-0.00000	0.22923
C6	0.28621	-0.00000	0.19544
C7	0.25469	-0.00000	0.19238
C8	0.37904	-0.00000	0.20267
C9	0.52259	-0.00000	0.30465
C10	0.52234	-0.00000	0.33696
C11	0.49363	-0.00000	0.37177
C12	0.46283	-0.00000	0.36759
C13	0.46308	-0.00000	0.33448
C14	0.49432	-0.00000	0.29865
N15	0.50025	-0.00000	0.25984
N16	0.49864	-0.00000	0.40495
C17	0.54003	-0.00000	0.22695
C18	0.46812	-0.00000	0.25229
C19	0.46612	-0.00000	0.44537
C20	0.53807	-0.00000	0.39766
C21	0.54704	-0.00000	0.19193
C22	0.57807	-0.00000	0.1593
C23	0.6106	-0.00000	0.15664
C24	0.60927	-0.00000	0.19066

C25	0.57582	-0.00000	0.22338
C26	0.43028	-0.00000	0.27831
C27	0.4014	-0.00000	0.27244
C28	0.40693	-0.00000	0.23868
C29	0.44136	-0.00000	0.2111
C30	0.46952	-0.00000	0.21777
C31	0.5744	-0.00000	0.3651
C32	0.60719	-0.00000	0.36503
C33	0.60712	-0.00000	0.39684
C34	0.57455	-0.00000	0.42731
C35	0.54413	-0.00000	0.42589
C36	0.46726	-0.00000	0.47858
C37	0.43926	-0.00000	0.51413
C38	0.40505	-0.00000	0.52181
C39	0.39938	-0.00000	0.49376
C40	0.42824	-0.00000	0.45811
N41	0.3772	-0.00000	0.23341
C42	0.70461	-0.00000	0.40021
C43	0.73418	-0.00000	0.40392
C44	0.73016	-0.00000	0.43828
C45	0.69636	-0.00000	0.46875
C46	0.66674	-0.00000	0.465
C47	0.67086	-0.00000	0.43075
C48	0.63911	-0.00000	0.4284
C49	0.7614	-0.00000	0.44185
N50	0.63933	-0.00000	0.39827
N51	0.6419	-0.00000	0.12453
C52	0.64327	-0.00000	0.09254
C53	0.76552	-0.00000	0.95263

C54	0.73527	-0.00000	0.989
C55	0.7396	-0.00000	0.01896
C56	0.70975	-0.00000	0.05342
C57	0.67576	-0.00000	0.05775
C58	0.67178	-0.00000	0.02772
C59	0.70129	-0.00000	0.99364
C60	0.31227	-0.00000	0.62275
C61	0.2813	-0.00000	0.65534
C62	0.28229	-0.00000	0.68718
C63	0.31496	-0.00000	0.68578
C64	0.34643	-0.00000	0.65261
C65	0.34496	-0.00000	0.62114
C66	0.3774	-0.00000	0.58663
N67	0.37567	-0.00000	0.55766
C68	0.03892	-0.00000	0.77778
C69	0.00858	-0.00000	0.77289
C70	0.97161	-0.00000	0.79908
C71	0.97471	-0.00000	0.82832
C72	0.00204	-0.00000	0.83621
C73	0.03769	-0.00000	0.81191
N74	0.0653	-0.00000	0.82496
N75	0.93172	-0.00000	0.80565
C76	0.10674	-0.00000	0.79854
C77	0.05068	-0.00000	0.86643
C78	0.8976	-0.00000	0.84394
C79	0.92587	-0.00000	0.77339
C80	0.1357	-0.00000	0.80641
C81	0.1725	-0.00000	0.78167
C82	0.18427	-0.00000	0.7461

C83	0.16012	-0.00000	0.73551
C84	0.12394	-0.00000	0.76054
C85	0.0137	-0.00000	0.89787
C86	0.0037	-0.00000	0.93385
C87	0.02955	-0.00000	0.94202
C88	0.06411	-0.00000	0.91602
C89	0.07334	-0.00000	0.88078
C90	0.95568	-0.00000	0.74177
C91	0.96247	-0.00000	0.70817
C92	0.93474	-0.00000	0.70226
C93	0.90051	-0.00000	0.73207
C94	0.89573	-0.00000	0.76702
C95	0.86288	-0.00000	0.84885
C96	0.83045	-0.00000	0.88096
C97	0.82951	-0.00000	0.91307
C98	0.86103	-0.00000	0.91231
C99	0.89341	-0.00000	0.87983
N100	0.22045	-0.00000	0.71908
N101	0.94128	-0.00000	0.66673
C102	0.03902	-0.00000	0.02645
C103	0.04811	-0.00000	0.05192
C104	0.02137	-0.00000	0.08745
C105	0.98733	-0.00000	0.09336
C106	0.97795	-0.00000	0.06736
C107	0.00276	-0.00000	0.03597
C108	0.99712	-0.00000	0.00317
C109	0.03108	-0.00000	0.11401
N110	0.0231	-0.00000	0.97661
N111	0.79749	-0.00000	0.9471

C112	0.97728	-0.00000	0.30566
C113	0.0072	-0.00000	0.27299
C114	0.04593	-0.00000	0.2636
C115	0.04261	-0.00000	0.29664
C116	0.01232	-0.00000	0.33132
C117	0.97559	-0.00000	0.33906
N118	0.94247	-0.00000	0.37838
N119	0.08522	-0.00000	0.22792
C120	0.90223	-0.00000	0.38812
C121	0.95016	-0.00000	0.40947
C122	0.12015	-0.00000	0.229
C123	0.08954	-0.00000	0.19002
C124	0.87039	-0.00000	0.42381
C125	0.83448	-0.00000	0.43301
C126	0.82639	-0.00000	0.4067
C127	0.85308	-0.00000	0.37242
C128	0.88843	-0.00000	0.3641
C129	0.98462	-0.00000	0.40665
C130	0.99148	-0.00000	0.43448
C131	0.96373	-0.00000	0.46866
C132	0.93005	-0.00000	0.47514
C133	0.92396	-0.00000	0.44695
C134	0.05904	-0.00000	0.19112
C135	0.04919	-0.00000	0.16693
C136	0.07466	-0.00000	0.13177
C137	0.11009	-0.00000	0.12336
C138	0.11784	-0.00000	0.15162
C139	0.15364	-0.00000	0.19692
C140	0.18698	-0.00000	0.19324

C141	0.19018	-0.00000	0.22301
C142	0.15974	-0.00000	0.25595
C143	0.12615	-0.00000	0.25925
N144	0.7916	-0.00000	0.4125
N145	0.2236	-0.00000	0.22118
N146	0.0644	-0.00000	0.10557
C147	0.95013	-0.00000	0.59859
C148	0.95608	-0.00000	0.56461
C149	0.99122	-0.00000	0.53504
C150	0.01815	-0.00000	0.5442
C151	0.01207	-0.00000	0.57865
C152	0.97914	-0.00000	0.60344
C153	0.97329	-0.00000	0.63873
C154	0.99655	-0.00000	0.49967
N155	0.96791	-0.00000	0.49833
C156	0.24882	-0.00000	0.72115
N157	0.42974	-0.00000	0.39405
S158	0.39766	-0.00000	0.38441
N159	0.43002	-0.00000	0.34188
N160	0.02248	-0.00000	0.73687
S161	0.06606	-0.00000	0.70956
N162	0.06832	-0.00000	0.74625
N163	0.94881	-0.00000	0.30358
S164	0.94997	-0.00000	0.26504
N165	0.99345	-0.00000	0.24656
H166	0.32257	-0.00000	0.13816
H167	0.37611	-0.00000	0.1427
H168	0.31031	-0.00000	0.25812
H169	0.25723	-0.00000	0.25366

H170	0.25817	-0.00000	0.16599
H171	0.40385	-0.00000	0.17754
H172	0.54715	-0.00000	0.28517
H173	0.54683	-0.00000	0.33165
H174	0.53008	-0.00000	0.18518
H175	0.57476	-0.00000	0.13639
H176	0.63437	-0.00000	0.19027
H177	0.58632	-0.00000	0.24056
H178	0.41547	-0.00000	0.30487
H179	0.37389	-0.00000	0.29465
H180	0.44641	-0.00000	0.18384
H181	0.48727	-0.00000	0.19008
H182	0.5855	-0.00000	0.33701
H183	0.63273	-0.00000	0.34011
H184	0.57082	-0.00000	0.4538
H185	0.52715	-0.00000	0.44973
H186	0.48446	-0.00000	0.48873
H187	0.44399	-0.00000	0.53646
H188	0.37187	-0.00000	0.49986
H189	0.41341	-0.00000	0.44662
H190	0.70814	-0.00000	0.37369
H191	0.76016	-0.00000	0.37973
H192	0.69291	-0.00000	0.49524
H193	0.64053	-0.00000	0.48893
H194	0.61529	-0.00000	0.45411
H195	0.75911	-0.00000	0.46781
H196	0.61985	-0.00000	0.09054
H197	0.76034	-0.00000	0.9309
H198	0.76587	-0.00000	0.01576

H199	0.71318	-0.00000	0.07636
H200	0.64564	-0.00000	0.03055
H201	0.69753	-0.00000	0.97088
H202	0.31042	-0.00000	0.59886
H203	0.25655	-0.00000	0.65526
H204	0.31607	-0.00000	0.71009
H205	0.37179	-0.00000	0.65148
H206	0.40199	-0.00000	0.58669
H207	0.99582	-0.00000	0.85612
H208	0.13998	-0.00000	0.82773
H209	0.19218	-0.00000	0.79001
H210	0.16985	-0.00000	0.70688
H211	0.11526	-0.00000	0.74393
H212	0.98863	-0.00000	0.90054
H213	0.97815	-0.00000	0.95134
H214	0.08442	-0.00000	0.92353
H215	0.09909	-0.00000	0.86967
H216	0.97464	-0.00000	0.74381
H217	0.99034	-0.00000	0.68813
H218	0.8778	-0.00000	0.7283
H219	0.8676	-0.00000	0.78318
H220	0.85707	-0.00000	0.82971
H221	0.80634	-0.00000	0.87977
H222	0.86011	-0.00000	0.93783
H223	0.90989	-0.00000	0.8913
H224	0.06109	-0.00000	0.99905
H225	0.07613	-0.00000	0.04362
H226	0.96652	-0.00000	0.12132
H227	0.95014	-0.00000	0.07496

H228	0.97045	-0.00000	0.00739
H229	0.00867	-0.00000	0.14073
H230	0.06473	-0.00000	0.29685
H231	0.02423	-0.00000	0.34551
H232	0.86419	-0.00000	0.44966
H233	0.81281	-0.00000	0.46081
H234	0.84513	-0.00000	0.35218
H235	0.89602	-0.00000	0.33776
H236	0.00845	-0.00000	0.39203
H237	0.01643	-0.00000	0.43378
H238	0.90816	-0.00000	0.50293
H239	0.89746	-0.00000	0.4618
H240	0.04214	-0.00000	0.21304
H241	0.02085	-0.00000	0.17813
H242	0.14616	-0.00000	0.13723
H243	0.15754	-0.00000	0.17252
H244	0.20998	-0.00000	0.16648
H245	0.16235	-0.00000	0.27952
H246	0.11033	-0.00000	0.28753
H247	0.92291	-0.00000	0.6209
H248	0.93283	-0.00000	0.56181
H249	0.04519	-0.00000	0.52157
H250	0.03465	-0.00000	0.58257
H251	0.99726	-0.00000	0.63977
H252	0.02078	-0.00000	0.48057
H253	0.2481	-0.00000	0.74635
H254	0.13133	-0.00000	0.09553
H255	0.95351	-0.00000	0.85112

Table S3. Unit cell parameters and fractional atomic coordinates for HIAM-0023 based on the AA-stacking.

Space group	CM		
Calculated unit cell	a = 32.2745 Å, b = 29.3605 Å, c = 4.7628 α = γ = 90°, β = 91.0557°		
C1	0.1214	0.52287	-0.03394
C3	0.15553	0.45344	0.07831
C4	0.1895	0.47782	0.18332
N7	0.15585	0.59385	0.07689
C9	0.1171	0.61822	0.07414
C10	0.19486	0.61774	0.05335
C13	0.11216	0.65322	-0.10939
C14	0.07548	0.67773	-0.10999
C15	0.04243	0.66876	0.07831
C16	0.04575	0.63332	0.26195
C17	0.08203	0.60774	0.26651
C18	0.22517	0.60526	-0.14289
C19	0.26383	0.6264	-0.15853
C20	0.27279	0.6615	0.02254
C21	0.24167	0.67518	0.21098
C22	0.20304	0.65371	0.22545
N33	0.31055	0.31772	0.02713
C35	-0.11263	0.7677	0.09239
C36	-0.07484	0.74416	0.12574
C37	-0.0395	0.75639	-0.03435
C38	-0.04228	0.79143	-0.22133
C39	-0.08	0.81467	-0.25649
C40	-0.11548	0.80235	-0.09895
C41	-0.15539	0.82645	-0.13473

C42	0.00124	0.7334	-0.01789
N43	0.00448	0.69412	0.07965
O53	-0.07059	0.29078	0.3154
O54	-0.08399	0.14997	-0.44378
C57	-0.04729	0.13329	-0.57813
C58	-0.10714	0.30718	0.45296
C59	-0.0593	0.09429	-0.75632
C60	-0.09493	0.34618	0.63048
N65	0.22513	0.46123	0.288
H68	0.09489	0.53956	-0.1261
H70	0.13676	0.66148	-0.25552
H71	0.07303	0.70333	-0.26422
H72	0.02028	0.62593	0.40484
H73	0.08459	0.58101	0.41263
H74	0.21895	0.57812	-0.27732
H75	0.28599	0.61446	-0.31143
H76	0.24765	0.70215	0.35132
H77	0.17985	0.66464	0.3745
H86	-0.14012	0.75928	0.21355
H87	-0.01468	0.79992	-0.34176
H88	-0.15641	0.85181	-0.2904
H89	0.02851	0.75	-0.10009
H94	-0.02394	0.12283	-0.4181
H95	-0.03329	0.15825	-0.71759
H96	-0.12077	0.28204	0.59282
H97	-0.13086	0.31756	0.29513
H98	-0.03116	0.08179	-0.8679
H99	-0.08335	0.1037	-0.914
H100	-0.07227	0.06819	-0.62065

H101	-0.08264	0.37241	0.49329
H102	-0.07023	0.33694	0.78381
H103	-0.1228	0.35835	0.74647
S66	0.25935	0.5	0.38993

Table S4. Unit cell parameters and fractional atomic coordinates for HIAM-0024 based on the AA-stacking.

Space group	CM		
Calculated unit cell	a = 30.7571 Å, b = 32.7385 Å, c = 4.6603 α = γ = 90°, β = 90.1773°		
C1	0.11489	0.52189	0.111
C2	0.14645	0.45537	-0.03928
C3	0.17798	0.47868	-0.18282
N4	0.14583	0.58995	-0.04343
C5	0.10527	0.61165	-0.02148
C6	0.18503	0.61458	-0.04135
C7	0.10075	0.64449	0.17291
C8	0.06279	0.6671	0.18952
C9	0.02822	0.65769	0.00723
C10	0.03191	0.62377	-0.17986
C11	0.07017	0.60095	-0.19503
C12	0.22156	0.60109	0.10722
C13	0.2585	0.62554	0.12056
C14	0.25964	0.6647	-0.0134
C15	0.22369	0.67813	-0.16607
C16	0.18663	0.65371	-0.17634
N17	0.29707	0.30921	-0.00631
C18	0.36939	0.25219	-0.02321
C19	0.40798	0.2292	-0.04736
C20	-0.05678	0.7404	0.12621
C21	0.43928	0.27345	0.3197
C22	0.40095	0.29561	0.34503
C23	0.36571	0.28516	0.17291
C24	0.32608	0.31028	0.19291

C25	-0.01504	0.71857	0.11602
N26	-0.01097	0.68134	0.0103
O27	0.41326	0.80377	-0.24331
O28	0.39738	0.67237	0.54695
C29	0.42408	0.63702	0.49501
C30	0.37604	0.82169	-0.37143
C31	0.39548	0.5995	0.43614
C32	0.38939	0.86006	-0.54161
N33	0.21108	0.46269	-0.3281
C34	0.42186	0.56119	0.36111
C35	0.3504	0.8837	-0.65283
H36	0.09016	0.53789	0.22972
H37	0.12705	0.65279	0.31027
H38	0.06085	0.69148	0.34784
H39	0.00541	0.61565	-0.31892
H40	0.07276	0.57562	-0.3459
H41	0.22178	0.57122	0.20878
H42	0.28619	0.61324	0.23136
H43	0.2241	0.70801	-0.27279
H44	0.15891	0.66593	-0.28497
H45	0.34216	0.24495	-0.15699
H46	0.46596	0.28174	0.45703
H47	0.32219	0.33071	0.37489
H48	0.0123	0.73461	0.20536
H49	0.44387	0.63119	0.68849
H50	0.4462	0.64168	0.31025
H51	0.35295	0.83102	-0.20246
H52	0.36068	0.79904	-0.51856
H53	0.37375	0.60665	0.25419

H54	0.37555	0.59285	0.62807
H55	0.40974	0.85045	-0.72509
H56	0.40856	0.88107	-0.40282
H57	0.44183	0.56714	0.16858
H58	0.3997	0.53522	0.31315
H59	0.44283	0.55226	0.54313
H60	0.33202	0.89702	-0.47093
H61	0.32908	0.86272	-0.77666
H62	0.36109	0.90943	-0.79401
S63	0.24329	0.5	-0.46464

Table S5. Unit cell parameters and fractional atomic coordinates for HIAM-0025 based on the AA-stacking.

Space group	CM		
Calculated unit cell	a = 31.7806 Å, b = 32.2379 Å, c = 4.4875 α = γ = 90°, β = 90.3228°		
C1	0.10593	0.52149	-0.28602
C2	0.13731	0.45598	-0.12393
C3	0.16872	0.479	0.03247
N4	0.13558	0.5887	-0.11417
C5	0.09363	0.60896	-0.13148
C6	0.1747	0.61394	-0.09642
C7	0.0886	0.64428	-0.30763
C8	0.04988	0.66616	-0.307
C9	0.01497	0.65341	-0.12571
C10	0.01855	0.61671	0.03538
C11	0.0576	0.59471	0.03343
C12	0.21395	0.60139	-0.22869
C13	0.25128	0.62549	-0.21156
C14	0.25029	0.66336	-0.06183
C15	0.2111	0.67708	0.05942
C16	0.17389	0.65276	0.04289
N17	0.28788	0.31079	-0.04183
C18	0.359	0.25327	-0.05905
C19	0.39476	0.22625	-0.07308
C20	-0.06298	0.74275	-0.08274
C21	0.44287	0.28506	-0.0568
C22	0.40742	0.3118	-0.02024
C23	0.36509	0.2958	-0.03592
C24	0.32757	0.32416	-0.03578

C25	-0.02333	0.71749	-0.1146
N26	-0.02359	0.67782	-0.09541
O27	0.38983	0.81659	-0.08409
O28	0.41247	0.64596	0.03805
C29	0.45529	0.63025	0.08125
C30	0.35046	0.83379	0.02954
C31	0.45269	0.58629	0.19714
C32	0.35666	0.87976	0.07096
N33	0.20148	0.46337	0.19358
C34	0.49611	0.5633	0.17742
C35	0.31549	0.89974	0.19725
C36	0.53465	0.5869	0.30801
C37	0.32211	0.94546	0.24673
H38	0.08074	0.53701	-0.40972
H39	0.11546	0.65591	-0.43566
H40	0.0476	0.69333	-0.4457
H41	-0.0083	0.60605	0.17233
H42	0.05992	0.56713	0.16555
H43	0.21614	0.57248	-0.34015
H44	0.2806	0.61465	-0.31981
H45	0.2094	0.70669	0.16834
H46	0.14422	0.6651	0.13212
H47	0.32629	0.24142	-0.06828
H48	0.47565	0.29682	-0.062
H49	0.33366	0.35675	-0.03246
H50	0.00725	0.73347	-0.14114
H51	0.47262	0.64864	0.25522
H52	0.47314	0.6312	-0.13702
H53	0.34235	0.82004	0.25297

H54	0.32364	0.82827	-0.13373
H55	0.42826	0.56919	0.06209
H56	0.44132	0.58662	0.43579
H57	0.36502	0.89374	-0.15077
H58	0.38414	0.885	0.22959
H59	0.50301	0.55516	-0.06156
H60	0.49267	0.53443	0.306
H61	0.3067	0.88535	0.41668
H62	0.28818	0.89519	0.03638
H63	0.54333	0.61296	0.15893
H64	0.56324	0.56633	0.32331
H65	0.52707	0.59856	0.53732
H66	0.29187	0.95908	0.33895
H67	0.32999	0.96069	0.02905
H68	0.34884	0.95088	0.41057
S69	0.23355	0.5	0.34373

Table S6. Summary of photocatalytic H_2O_2 production using COFs as photocatalysts.

Entry	COFs	Condition	Light source	H_2O_2 (μmol/g/h)	Ref.
1	TpAQ-COF	Water, O_2	300 W Xe lamp (λ > 420 nm)	420	1
2	TD-COF	Water, O_2	White LED (400-700nm)	4620	2
		Water, air		4060	
		Seawater, air		3364	
3	FS-COF	Water, O_2	300 W Xe lamp (λ > 420 nm)	3904	3
4	Py-Da-COF	Water, O_2	300 W Xe lamp (λ > 420 nm)	461	4
		Water/EtOH (9/1), O_2		682	
5	PMCR-1	Water, air	300 W Xe lamp (420-700 nm)	1294	5
		Water, O_2		1445	
		Water/BA (10/1), O2		5499	
6	TDB-COF	Water, air	AM 1.5	231	6
		Water, O_2		723.5	
		Water/EtOH(9/1), O2		1000.1	
7	COF-N32	Water, O_2	300 W Xe lamp (λ > 420 nm)	605	7
8	COF-2CN	Water, O_2	300 W Xe lamp (λ > 420 nm)	1601	8
9	COF-TfpBpy	Water, air	300 W Xe lamp (λ > 420 nm)	2084	9
10	TaptBtt	Water, air	300 W Xe lamp AM 1.5G	1407	10
11	DETH-COF	Water, air	300 W Xe lamp (λ > 420 nm)	1012	11
		Water, O_2		1665	
12	TTF-BT-COF	Water, O_2	300 W Xe lamp (λ > 420 nm)	2760	12
13	NiPc-THHI-COF	Water, O_2	300 W Xe lamp (λ > 400 nm)	4589	13
14	Fs-OHOMe-COF	Water, air	300 W Xe lamp (λ > 400 nm)	2200	14
15	PTA@TTB-EB	Water, O_2	300 W Xe lamp (λ > 420 nm)	897.94	15
16	4PE-N-S	Water, O_2	300 W Xe lamp	1574	16

			(420-700 nm)		
17	TTA-CTP-COF	Water, O_2	Full spectrum	520	17
18	TAPT-PDA-COF	Water/IPA (9/1), O_2	300 W Xe lamp ($\lambda > 420$ nm)	706.2	18
19	EBA-COF	Water/EtOH(9/1), O_2	50 W LED lamp (~ 420 nm)	1830	19
20	TAPB-PDA-OH	Water, O_2	10 W LED lamp ($\lambda > 420$ nm)	1841.3	20
		Water/EtOH(9/1), O_2		2177.6	
21	DMCR-1NH	Water/IPA (10/1), O_2	300 W Xe lamp (420-700 nm)	2588	21
		Water/IPA (10/1), air		2264.5	
22	TF_{50}-COF	Water/EtOH (9/1), O_2	300 W Xe lamp ($\lambda > 400$ nm)	1739	22
23	COF-NUST-16	Water/EtOH(9/1), O_2	300 W Xe lamp ($\lambda > 420$ nm)	1081	23
24	TAPT-TFPA COFs@Pd ICs	Water/EtOH(9/1), O_2	300 W Xe lamp AM 1.5	2143	24
25	TPB-DMTP-COF	Water/EtOH/5wt.% PTFE, air	300 W Xe lamp ($\lambda > 420$ nm)	2882	25
26	COF-TAPB-BPDA	Water/BA (4/1), O_2	300 W Xe lamp ($\lambda > 420$ nm)	1240	26
27	COF-BTT-TAPT	Water/EtOH(1/9), O_2	300 W Xe lamp ($\lambda > 420$ nm)	620	27
28	Bpy-TAPT	Water, O_2	300 W Xe lamp ($\lambda > 420$ nm)	4038	28
29	TAPT-BT-COF	Water, O_2	300 W Xe lamp ($\lambda > 420$ nm)	1360 ± 30	29
30	DQTb-COFs	Water, O_2	300 W Xe lamp ($\lambda > 400$ nm)	1844	30
31	HEP-TAPT-COF	Water, O_2	300 W Xe lamp ($\lambda > 420$ nm)	1750	31
32	TpDz	Water, O_2	300 W Xe lamp ($\lambda > 420$ nm)	7327	32
33	TAPD-$(Me)_2$ COF	Water/EtOH(9/1), O_2	300 W Xe lamp (420-700 nm)	97	33
		Water/EtOH(1/9), O_2		234.5	
34	TP-$DPBD_{3O}$-	Water, air	300 W Xe lamp ($\lambda > 300$ nm)	9200	34

			300 W Xe lamp (420-600 nm)	7200	
		Water, O_2		8100	
35	COF@H_3PO_4	Water, O_2	300 W Xe lamp ($\lambda > 420$ nm)	5214	35
36	H_2Se-COF	Water/BA(9/1), O_2	300 W Xe lamp ($\lambda > 420$ nm)	6145	36
37	HCOF	Water, O_2	300 W Xe lamp ($\lambda \geqslant 420$ nm)	2113.9	37
38	TTF-PDI-COF	Water/BA(9/1), O_2	LED lamp (~ 420 nm)	3600	38
39	TPB-COF-OH	Water, air	300 W Xe lamp ($\lambda \geqslant 420$ nm)	6608	39
40	TBD-COF	Water, O_2	white LED (400-700 nm)	6085	40
		Water, air		5448	
41	PyIm-COF	Water, O_2	300 W Xe lamp ($\lambda > 420$ nm)	5850	41
42	DVA-COF	Water/BA(9/1), O_2	LED lamp (~ 420 nm)	8450	42
43	Kf-AQ	Water, O_2 (pH = 13)	300 W Xe lamp ($\lambda > 400$ nm)	4784	43
44	TBTN-COF	Water, O_2	300 W Xe lamp ($\lambda > 420$ nm)	11013	44
45	TB-COF	Water, air	white LED (400-700 nm)	5186	45
46	p-COF-TpPzda	Water, O_2	300 W Xe lamp ($\lambda > 420$ nm)	6434	46
47	20COFIS	Water, air	360 W Xe lamp	5713.15	47
48	Hz-TP-BT-COF	Water, air	300 W Xe lamp (420-600 nm)	5700	48
		Water, O_2		6500	
		Water, air	300 W Xe lamp ($\lambda > 300$ nm)	12500	
49	SO_3H-COF	Water, O_2	300 W Xe lamp ($\lambda > 400$ nm)	3015	49
		Water/MeOH(9/1), O_2		4971	
50	HIAM-0022	Water, air	300 W Xe lamp ($\lambda > 420$ nm)	68.89	This work
	HIAM-0023			149.51	
	HIAM-0024			86.09	
	HIAM-0025			70.06	
	HIAM-0023-12.5%			264.02	
	HIAM-0023-25%			307.33	

	HIAM-0023-37.5%			391.66	
	HIAM-0023-50%			246	

References

1. Zhang, X.; Zhang, J.; Miao, J.; Wen, X.; Chen, C.; Zhou, B.; Long, M. *Chem. Eng. J.* **2023**, 466, 143085.

2. Yue, J. Y.; Song, L. P.; Fan, Y. F.; Pan, Z. X.; Yang, P.; Ma, Y.; Xu, Q.; *Angew. Chem. Int. Ed.* **2023**, 62, e202309624.

3. Luo, Y.; Zhang, B.; Liu, C.; Xia, D.; Ou, X.; Cai, Y.; Zhou, Y.; Jiang, J.; Han, B. *Angew. Chem. Int. Ed.* **2023**, 62, e202305355.

4. Sun, J.; Sekhar Jena, H.; Krishnaraj, C.; Singh Rawat, K.; Abednatanzi, S.; Chakraborty, J.; Laemont, A.; Liu, W.; Chen, H.; Liu, Y. Y.; *Angew. Chem. Int. Ed.* **2023**, 62, e202216719.

5. Das, P.; Roeser, J.; Thomas, A. *Angew. Chem. Int. Ed.* **2023**, 62, e202304349.

6. Zhou, Z.; Sun, M.; Zhu, Y.; Li, P.; Zhang, Y.; Wang, M.; Shen, Y. *Appl. Catal. B. Environ.* **2023**, 334, 122862.

7. Liu, F.; Zhou, P.; Hou, Y.; Tan, H.; Liang, Y.; Liang, J.; Zhang, Q.; Guo, S.; Tong, M.; Ni, *Nat. Commun.* **2023**, 14, 4344.

8. Hou, Y.; Zhou, P.; Liu, F.; Lu, Y.; Tan, H.; Li, Z.; Tong, M.; Ni, J. *Angew. Chem. Int. Ed.* **2023**, 63, e202318562.

9. Kou, M.; Wang, Y.; Xu, Y.; Ye, L.; Huang, Y.; Jia, B.; Li, H.; Ren, J.; Deng, Y.; Chen, J.; *Angew. Chem. Int. Ed.* **2022**, 61, e202200413.

10. Qin, C.; Wu, X.; Tang, L.; Chen, X.; Li, M.; Mou, Y.; Su, B.; Wang, S.; Feng, C.; Liu, J.; *Nat. Commun.* **2023**, 14, 5238.

11. Pan, G.; Hou, X.; Liu, Z.; Yang, C.; Long, J.; Huang, G.; Bi, J.; Yu, Y.; Li, L. *ACS. Catal.* **2022**, 12, 14911-14917.

12. Chang, J. N.; Li, Q.; Shi, J. W.; Zhang, M.; Zhang, L.; Li, S.; Chen, Y.; Li, S. L.; Lan, Y. Q. *Angew. Chem. Int. Ed.* **2023**, 63, e202218868.

13. Wang, X.; Jin, Y.; Li, N.; Zhang, H.; Liu, X.; Yang, X.; Pan, H.; Wang, T.; Wang, K.; Qi, D.; *Angew. Chem. Int. Ed.* **2024**, 63, e202401014.

14. Shu, C.; Yang, X.; Liu, L.; Hu, X.; Sun, R.; Yang, X.; Cooper, A.; Tan, B.; Wang, X. *Angew. Chem. Int. Ed.* **2024**. 63, e202403926.

15. Rong, Q.; Chen, X.; Li, S.; He, S. *ACS. Appl. Mater. Interfaces.* **2024**. 16, 5758-5768

16. Deng, M.; Sun, J.; Laemont, A.; Liu, C.; Wang, L.; Bourda, L.; Chakraborty, J.; Van Hecke, K.; Morent, R.; De Geyter, N. *Green. Chem.* **2023**, 25, 3069-3076.

17. Liao, J.-P.; Zhang, M.; Huang, P.; Dong, L.-Z.; Ma, T.-T.; Huang, G.-Z.; Liu, Y.-F.; Lu, M.; Li, S.-L.; Lan, Y.-Q. *ACS. Catal* .**2024**, 3778-3787.

18. Zhou, S.; Hu, H.; Hu, H.; Jiang, Q.; Xie, H.; Li, C.; Gao, S.; Kong, Y.; Hu, Y. *Sci. China Mater.* **2023**, 66, 1837-1846.

19. Zhai, L.; Xie, Z.; Cui, C.-X.; Yang, X.; Xu, Q.; Ke, X.; Liu, M.; Qu, L.-B.; Chen, X.; Mi, L. *Chem. Mater.* **2022**, 34, 5232-5240.

20. Yang, Y.; Kang, J.; Li, Y.; Liang, J.; Liang, J.; Jiang, L.; Chen, D.; He, J.; Chen, Y.; Wang, J. *New J. Chem.* **2022**, 46, 21605-21614.

21. Das, P.; Chakraborty, G.; Roeser, J.; Vogl, S.; Rabeah, J.; Thomas, A. *J. Am. Chem. Soc.* **2023**, 145, 2975-2984.

22. Wang, H.; Yang, C.; Chen, F.; Zheng, G.; Han, Q. *Angew. Chem. Int. Ed.* **2022**, 61, e202202328.

23. Wu, M.; Shan, Z.; Wang, J.; Liu, T.; Zhang, G. *Chem. Eng. J.* **2023**, 454, 140121.

24. Liu, Y.; Li, L.; Tan, H.; Ye, N.; Gu, Y.; Zhao, S.; Zhang, S.; Luo, M.; Guo, S. *J. Am. Chem. Soc.* **2023**, 145, 19877-19884.

25. Li, L.; Xu, L.; Hu, Z.; Yu, J. C. *Adv. Funct. Mater.* **2021**, 31, 2106120.

26. Yang, T.; Chen, Y.; Wang, Y.; Peng, X.; Kong, A. *ACS. Appl. Mater. Interfaces.* **2023**, 15, 8066-8075.

27. Liu, M.; He, P.; Gong, H.; Zhao, Z.; Li, Y.; Zhou, K.; Lin, Y.; Li, J.; Bao, Z.; Yang, Q.; *Chem. Eng. J.* **2024**, 482, 148922.

28. Liu, Y.; Han, W.-K.; Chi, W.; Mao, Y.; Jiang, Y.; Yan, X.; Gu, Z.-G. *Appl. Catal. B.* **2023**, 331, 122691.

29. Wang, L.; Sun, J.; Deng, M.; Liu, C.; Ataberk Cayan, S.; Molkens, K.; Geiregat, P.; Morent, R.; De Geyter, N.; Chakraborty, J.; *Catal .Sci Technol.* **2023**, 13, 6463-6471.

30. Luo, Y.; Liu, C.; Liu, J.; Liu, X.; Zhou, Y.; Ou, X.; Weng, B.; Jiang, J.; Han, B. *Chem. Eng. J.* **2024**, 481, 148494.

31. Chen D, ; Chen W, ; Chen L; Angew. Chem. Int. Ed, **2023**, 62, e202217479.

32. Liao, Q.; Sun, Q.; Xu, H.; Wang, Y.; Xu, Y.; Li, Z.; Hu, J.; Wang, D.; Li, H.; Xi, K. *Angew. Chem. Int. Ed.* **2023**, 62, e202310556.

33. Krishnaraj, C.; Sekhar Jena, H.; Bourda, L.; Laemont, A.; Pachfule, P.; Roeser, J.; Chandran, C. V.; Borgmans, S.; Rogge, S. M. J.; Leus, K.; *J. Am. Chem. Soc.* **2020**, 142, 20107-20116.

34. Chen, Y.; Liu, R.; Guo, Y.; Wu, G.; Sum, T. C.; Yang, S. W.; Jiang, D. *Nat. Synth.* **2024**, 1-13.

35. Lin, Y.; Zou, J.; Wu, X.; Tong, S.; Niu, Q.; He, S.; Luo, S.; Yang, C. *Nano. Letters.* **2024**, 24, 6302-6311.

36. Dong, P.; Xu, X.; Wu, T.; Luo, R.; Kong, W.; Xu, Z.; Yuan, S.; Zhou, J.; Lei, J. *Angew. Chem. Int. Ed.* **2024**, 63, e202405313.

37. Zhu, Q.; Shi, L.; Li, Z.; Li, G.; Xu, X. *Angew. Chem. Int. Ed.* **2024**, 63, e202408041.

38. Xu, H.; Xia, S.; Li, C.; Li, Y.; Xing, W.; Jiang, Y.; Chen, X. *Angew. Chem. Int. Ed.* **2024**, 63, e202405476.

39. Feng, S.; Cheng, H.; Chen, F.; Liu, X.; Wang, Z.; Xu, H.; Hua, J. *ACS. Catalysis.* **2024**, 14, 7736-7745.

40. Yue, J. Y.; Luo, J. X.; Pan, Z. X.; Zhang, R. Z.; Yang, P.; Xu, Q.; Tang, B. *Angew. Chem. Int. Ed.* **2024**, 63, e202405763.

41. Wu, W.; Li, Z.; Liu, S.; Zhang, D.; Cai, B.; Liang, Y.; Wu, M.; Liao, Y.; Zhao, X. *Angew. Chem. Int. Ed.* **2024**, 63, e202404563.

42. Yu, H.; Zhang, F.; Chen, Q.; Zhou, P. K.; Xing, W.; Wang, S.; Zhang, G.; Jiang, Y.; Chen, X. *Angew. Chem. Int. Ed.* **2024**, 63, e202402297.

43. Zhang, X.; Cheng, S.; Chen, C.; Wen, X.; Miao, J.; Zhou, B.; Long, M.; Zhang, L. *Nat. Commun.* **2024**, 15, 2649.

44. Zhou, E.; Wang, F.; Zhang, X.; Hui, Y.; Wang, Y. *Angew. Chem. Int. Ed.* **2024**, 63, e202400999.

45. Yue, J.-Y.; Song, L.-P.; Pan, Z.-X.; Yang, P.; Ma, Y.; Xu, Q.; Tang, B. *ACS. Catalysis.* **2024**, 14, 4728-4737.

46. Yang, T.; Zhang, D.; Kong, A.; Zou, Y.; Yuan, L.; Liu, C.; Luo, S.; Wei, G.; Yu, C. *Angew. Chem. Int. Ed.* **2024**, 63, e202404077.

47. Qiu, J.; Meng, K.; Zhang, Y.; Cheng, B.; Zhang, J.; Wang, L.; Yu, J. *Adv. Mater.* **2024,** 2400288.

48. Liu, R.; Chen, Y.; Yu, H.; Položij, M.; Guo, Y.; Sum, T. C.; Heine, T.; Jiang, D. *Nat. Catal,* **2024**, 7, 195-206.

49. Li, L.; Lv, X.; Xue, Y.; Shao, H.; Zheng, G.; Han, Q. Angew. Chem. Int. Ed, **2024**, 63, e202320218.